12-2021

# Development of Vegetable Oil-Based Nano-Lubricants Using Montmorillonite Clay (MMT) Nanoparticles as Lubricant Additives

Md Mashfiqur Rahman
*The University of Texas Rio Grande Valley*

# DEVELOPMENT OF VEGETABLE OIL-BASED NANO-LUBRICANTS USING MONTMORILLONITE CLAY (MMT) NANOPARTICLES AS LUBRICANT ADDITIVES

A Thesis

by

MD MASHFIQUR RAHMAN

Submitted in Partial Fulfillment of the

Requirements for the Degree of

MASTER OF SCIENCE IN ENGINEERING

Major Subject: Mechanical Engineering

The University of Texas Rio Grande Valley

December 2021

# DEVELOPMENT OF VEGETABLE OIL-BASED NANO-LUBRICANTS USING MONTMORILLONITE CLAY (MMT) NANOPARTICLES AS LUBRICANT ADDITIVES

A Thesis

by

MD MASHFIQUR RAHMAN

COMMITTEE MEMBERS

Dr. Javier A. Ortega
Chair of Committee

Dr. Horacio Vasquez
Committee Member

Dr. Arturo Fuentes
Committee Member

December 2021

ABSTRACT

Rahman, MD Mashfiqur, Development of Vegetable Oil-based Nano-lubricants using Montmorillonite Clay (MMT) Nanoparticles as Lubricant Additives. Master of Science in Engineering (MSE), December 2021, 86 pp., 7 Tables, 42 Figures, 30 References.

Because of the environmental impact and price volatility, there has been a growing concern on the use of petroleum-based lubricants. This issue has stimulated research into the development of biodegradable lubricants like vegetable oils. In this study, the tribological and rheological behavior of sunflower, peanut, and corn oils modified with Montmorillonite nanoclay (MMT) as lubricant additives were evaluated. A block-on-ring tribotester was used to evaluate the wear and friction characteristics of the nano-lubricants. Using a parallel plate rheometer, the effects of concentration and shear rate on shear viscosity were investigated. A custom-made tapping torque tester was used to evaluate the nano-lubricants in a real-world application. It was found that the volumetric wear, COF, and torque of the system decreased when MMT nanoparticles were added. The newly developed vegetable oil-based nano-lubricants with the addition of MMT nanoclay, look like a promising environmentally friendly solution to compete with petroleum-based lubricants.

# DEDICATION

This thesis work is dedicated to my mother, Nilufar Begum, who has always loved me unconditionally and whose good examples has taught me to work hard for the things that I aspire to achieve. This work is also dedicated to my wife, Oishe, my two elder sisters (Sony and Labony), and my mother-in-law who have been a constant source of support and encouragement during the challenges of graduate school and life. The completion of my master's studies here at UTRGV would not have been possible without the love and support of my family and close friends. Thank you very much for all the mental support, love, and patience you have provided.

# ACKNOWLEDGMENT

I would like to acknowledge my supervisor, Dr. Javier Ortega, for his outstanding guidance and support. His knowledge, expertise and his ongoing mentorship have helped me overcome all the difficulties I faced during this master's program. I am delighted that I got the opportunity to work in the Mechanical Engineering Faculty Research Lab under his supervision. I have found no words enough to show my gratitude towards him. Besides, I am very thankful to Dr. Karen Lozano, Dr. Victoria M. Padilla, and Dr. M. Jasim Uddin. I would specially mention Dario Rodriguez as his continuous learning mentality, and industriousness motivated me a lot. I have learned a lot from Dario Rodriguez, as he has excellent experience in this field. I want to thank Mohammad Anis, Apu Deb, Shunondo, Provashish Roy, Riyad Hossain, Jony De Sparrow, Nizamul Nibir, Arafat Hossain, Shishir Barai, Shuvendu Das, Shamim Hossain, Saumik Sakib for making my journey smooth at the earlier stage. I am also thankful to my colleague, Md. Abu Sayeed Biswas for his continuous encouragement and support.

TABLE OF CONTENTS

Page

LIST OF TABLES

Page

LIST OF FIGURES

Page

# CHAPTER I

# INTRODUCTION

## 1.1 Problem Statement

The concept of lubrication isn't new, it's one of the oldest forms of technology which dates back in the archaeological periods. Lubrication is the process or technique of applying lubricant to reduce friction and wear between two relative moving surfaces. The main purpose of using lubricant is to minimize the wear and friction in machinery (bearing, shaft) and protect the mechanical parts from failure. Mineral oil, refined from the fraction distillation of crude oil, has been used as a lubricant for a long time but it has some adverse effect in both health and environment. Synthetic oil which is manufactured by petroleum products can also be a good option, but it is not eco-friendly as well. So, the main concern is to reduce the amount of pollution and find something environmentally friendly. This concern has led the researchers to find an alternative way such as biodegradable vegetable oils. Moreover, the depletion of fossil fuels, the fluctuation of petroleum prices and growing concerns around environmental health, has promoted an interest towards biodegradable lubricants as well. Replacement of mineral and petroleum-based oils through vegetable oils has been considered as an effective solution regarding these issues.

## 1.2 Purpose Statement

There is an increasing concern over the number of pollutions being released into the environment. Because of these reasons, significant focus has shifted towards biodegradable lubricants instead of those mineral and petroleum-based ones. Additives can be used to increase the tribological properties further, although most antiwear and extreme pressure additives contain phosphorus and chlorine chemicals, which are harmful to the environment. Due to their ecologically benign nature, nanoparticles are being investigated as lubricant additives in order to reduce wear and friction of the system. During this study, the effects of Montmorillonite nonclay (MMT) nanoparticles as lubricant additives into biodegradable vegetable oils will be investigated.

## 1.3 Research Objectives

The main goal of this research is to inspire and encourage future researchers to develop new low-cost, environmentally friendly nanomaterial-based nanolubricants. In the present work, the lubrication performance of vegetable oils (sunflower, peanut, and corn) altered by the addition of MMT (Montmorillonite) nanoparticles at various concentrations will be studied. In this study, the tribological (COF and wear volume loss) and rheological (viscosity) performance of the lubricants will be evaluated to determine how the addition of nanoparticles at different concentrations will affect these properties. Surface characterization of the MMT nanoparticles will be done by scanning electron microscopy (SEM), x-ray diffraction (XRD), thermogravimetric analysis (TGA). The morphology of the worn surfaces will be done by SEM and profilometer. Moreover, tapping torque test will be performed to see the real-life applications of this vegetable oil-based nanolubricants.

## 1.4 Thesis Organization

This thesis manuscript is organized into five chapters. The first chapter presents the background of the topic of interest, describes the research questions, assumptions, and objectives. The second chapter is a review of the literature focusing primarily on background of lubricants, lubricant additives, and lubrication mechanisms. The full experimental set-up along with the materials processing, testing procedures are described in the third chapter. All the experimental findings are described and discussed in the fourth chapter. Finally, chapter five provides a conclusion of the research work.

# CHAPTER II

# LITERATURE REVIEW

## 2.1 Background on Lubricants

Lubrication technology has advanced significantly in recent times, but the roots of lubrication extend back further than that. It is one of the oldest forms of technology in the history of human being. Archaeological evidence suggests that lubrication was used in ancient Egypt at least as far back as the 17th century BC [1]. During this time, olive oil was used as a lubricant to move large stones and other heavy objects. At 14$^{th}$ century BC, animal fats (tallow) were used by ancient Egyptians to lubricate chariot axels [1]. Animal fats and water were used as lubricants during the times of the Egyptians to assist with the creation of the pyramids [2]. During the early development of technology, vegetable oils were used in machinery and vehicles until the petroleum-based oils were discovered. The use of vegetable oils and animal fats for lubrication purposes had been practiced for many years. With the discovery of petroleum and the availability of inexpensive oils, alternatives became unattractive and were left by the wayside. Oil was discovered in Titusville, Pennsylvania, in 1859, marking the beginning of the petroleum era. This was the first successful oil well drilling in the United States.

Until this point, lubricants were primarily derived from animal fats and vegetable oils. [1]. This discovery led to petroleum surpassing animal fats and vegetable-based lubricants, as it displayed better performance and was also cheap [3]. In response to increased demand, notably

from the booming car industry, lubricant producers began treating their petroleum-based oils in the 1920s to improve lubricant performance (which had previously been very poor) [1]. A solvent refining method was invented in the 1920s and the use of additives to inhibit oxidation, resist corrosion, enhance the performance of lubricants proliferated across the industries in the 1930s [4]. From the 1940s, additives were used extensively in lubricant formulations, especially to prolong the performance and service life of automotive engine oils [1]. Synthetic lubricants were invented in the 1950s, particularly for the aviation and aerospace sectors [1]. Attention was refocused on vegetable oils during wartime and oil shortage situations. Vegetable oils were used as fuel, lubricants, greases, and energy transfer materials throughout World War I and World War II, to name a few instances. In addition, the 1973 oil embargo drew much-needed attention to the need for alternatives to petroleum-based fuels.

Nowadays, the amount of pollution being released into the environment has become a growing concern. Moreover, petroleum has been fluctuating in prices as the amount of fossil fuels are decreasing at a great extent. These problems have created a need to look at different types of cleaner oils. A growing interest in vegetable oil-based lubricants has emerged during the past two decades, coinciding with a rise in environmental awareness. Various mandates and regulations were imposed on petroleum products in Europe during the 1980s, resulting in the adoption of biodegradable lubricants as a result of these policies. During the 1990s, a large number of American corporations began manufacturing items that were biodegradable. At present, biodegradable lubricants are being investigated for their non-toxic and renewable nature, as well as having characteristics of lubricity on par or better than those of mineral based oils [5]. According to studies, though vegetable oils have the physical properties, they lack the thermo oxidation properties for extremely high temperatures [6]. Currently, the addition of

nanoparticles into the vegetable lubricants is being investigated as it could provide a possibility in elevating these lubricants to the levels of those of petroleum-based lubricants. It has been demonstrated that vegetable oil-based nanolubricants that have been enhanced with optimal concentrations of nanoparticles have wear and friction reduction capabilities comparable to those of conventional lubricants [5].

### 2.2 Vegetable Oils as Biodegradable Lubricants

Biodegradable lubricant oil has been more popular in recent years because of price fluctuations, regulatory challenges, and environmental concerns. Recently, significant focus has shifted towards vegetable oils, such as sunflower oil, peanut oil, corn oil, coconut oil, grapeseed oil, jojoba oil, soybean oil, and canola oil, among others. Vegetable oils possess high lubricity, a high viscosity index, and low volatility, which are excellent lubricating properties. They have become popular because of their biodegradability and non-toxicity as well. Since poor oxidation is a major disadvantage of vegetable oils, efforts have been made to improve thermo-oxidation. The free radical process causes oxidation in vegetable oils, which can be decreased by lowering free fatty acids. Again, vegetable oils have limited range of viscosity and poor properties at low temperature. Vegetable oils are biodegradable, less harmful in general, renewable, and minimize reliance on imported petroleum oils. As previously mentioned, vegetable oils have the capability of being able to provide the necessary requirements for use in metal cutting processes and even in machinery. In their natural state, vegetable oils can and have been used as lubricants. On the positive side, as compared to mineral oil, vegetable oils can provide superior lubricity. Another noteworthy feature of vegetable oil is their high flash/fire points; soybean oil has a flash point of 610°F (326°C), whereas mineral oils have a flash point of around 392°F (200°C). Another main attraction to these oils is their natural esters that can provide a natural attraction to metals [6].

They also contain palmitic, oleic, and linoleic acids that are very beneficial in the tribological process [7]. Three vegetable oils that are being looked at, as well as being studied in this project is that of sunflower, peanut, and corn oils as possible substitutes. Table 1 shows the fatty acid composition of some of the vegetable oils.

**Table 1:** Fatty acid composition of vegetable oils [8].

| Types | Fatty Acid | | | | | | |
|---|---|---|---|---|---|---|---|
| | 14:0 | 16:0 | 16:1 | 18:0 | 18:1 | 18:2 | 18:3 |
| Cottonseed | 1.1 | 27.3 | 1.4 | 3.1 | 16.7 | 50.4 | |
| Linseed | | 6.5 | | 4.5 | 19.5 | 16.5 | 53.0 |
| Palm | 1.0 | 43.1 | 0.2 | 4 | 39 | 10 | 0.2 |
| Sunflower | | 6.1 | | 3 | 27 | 64 | |
| Soyabean | | 12 | | 3.6 | 23.7 | 51.4 | 8.8 |
| Peanut | | 9.8 | 0.4 | 3.7 | 60.9 | 18.1 | |
| Corn | | 10.6 | | 26.7 | 59.8 | 0.9 | |

### 2.2.1 Sunflower Oil

Sunflower oil has been considered now a days as a substitute for mineral oil–based lubricants because of its natural and environmentally friendly characteristics**.** Under low loads, sunflower oil can show adequate tribological characteristics (antifriction and antiwear) compared with petroleum oil-based lubricants [9]. Sunflower oil is readily available, eco-friendly, and can be renewable sometimes. It consists of 59% polyunsaturated fat, linoleic acid, and 30% monounsaturated fat, oleic acid. Compared to other vegetable oils, the oleic acid concentration of sunflower oil is high which is beneficial in having good oxidation properties [6]. Moreover, high concentration of palmitic acid in sunflower oil is beneficial to improve the friction properties [7]. Sunflower is one of the vegetable oils with a high smoking point, being able to reach a smoke point temperature of about 227℃ [10]. Further research on sunflower oil needs to be done to

improve its oxidation properties through lubricant additives before it can be used as a substitute of other oils.

### 2.2.2 Peanut Oil

Compared to other available vegetable oils, it contains higher concentrations of palmitic acid as well as oleic acid [10] which is very beneficial in improving the tribological (Wear and friction) properties. Like sunflower oil, peanut oil seems to have a higher smoke point of about 230℃ [11]. Peanut oil is readily available, eco-friendly and can be renewable as well. For this reason, peanut oil can be viewed as a potential candidate as a substitution. But, before using it as a substitute of other oils, further research needs to be done to increase its oxidation properties.

### 2.2.3 Corn Oil

Corn oil contains higher concentrations of palmitic acid as well as linoleic acid compared to other vegetable oils which is responsible for their improved tribological properties [10]. Like the previous ones, the smoke point of corn oil is high as well, being able to reach a smoke point temperature of about 230℃ [12]. Moreover, corn oil is eco-friendly and readily available and that's why it can be considered as a potential candidate to substitute other oils. But the main concern is its oxidation property which can be improved through lubricant additives by further research.

## 2.3 Nanoparticles as Lubricant Additives

Lubricant is a substance (often a liquid) that improves the tribological properties by reducing the friction and wear when introduced between two moving surfaces. A lubricant creates a protective coating between two surfaces that are in contact, allowing the surfaces to be separated and the friction between them to be reduced. To improve the lubrication performance, additives have been used as anti-wear, extreme pressure, viscosity control, film-forming, and

deposit control additives because of their unique properties when compared to their bulk counterparts [6]. But the fact is, anti-wear and extreme pressure additives have some adverse effect in environment because they are basically phosphorus and chlorine compounds.

It has received considerable achievements by many researchers to apply nanoparticles as the lubricant additives to improve the anti-friction and wear resistance capability because they are eco-friendly. The use of nanoparticles in lubricants have been shown to result in great tribological properties. Recently, much attention has been given towards nanoparticles. Many studies have been conducted so far regarding the effects of nanoparticles as lubricant additives to improve the tribological performance by reducing friction and wear.

### 2.3.1 Types of Nanoparticles

Different types of nanoparticles have been investigated to use as lubricant additives in recent years which we found at several studies. These nanoparticles were fallen into five different categories based on their size, morphology, characteristic chemical elements, and they exhibited various effects on frictional surfaces.

Sulfides, Metals, Oxides, Nanocomposites, and Rare Earth Compounds are currently the five categories in which nanoparticles can be classified.

Due to their small size, higher surface area, metallic nanoparticles can show excellent tribological properties and self-repairing functions as lubricant additives. With the formation of tribofilms, the surface properties will be altered, and two friction surfaces will be separated, resulting in promising tribological performance [13]. Metallic nanoparticles also roll between two frictional surfaces which reduce the friction and wear significantly. Various types of metallic nanoparticles are used as lubricant additives such as Ti, Ni, Cu, Sn, Ag, Bi, Fe etc.

Metal oxide nanoparticles have a similar lubricating mechanism to metallic NPs, with rolling, sintering, and repair effects, as well as tribofilm production. Different types of metal oxides have been used as lubricant additives, including $TiO_2$, CuO, ZnO, $Al_2O_3$, $Fe_3O_4$, $ZnAl_2O_4$.

Metal sulfides, such as $MoS_2$, $WS_2$, FeS, and CuS, have been used as solid or liquid lubricant additives for decades. Under dry sliding condition, coefficient of friction and wear can be significantly reduced with the addition of metal sulfides and they exhibit anti friction behavior.

Nanocomposites are basically multi component materials that includes $Cu/SiO_2$, Cu/graphene oxide, $Al_2O_3/SiO_2$, serpentine/$La(OH)_3$, $Al_2O_3/TiO_2$. Nanocomposites typically exhibit better tribological performance than single nanoparticles because of their synergistic effect.

The lubrication mechanism of rare earth compounds includes the formation of a tribofilm and absorption film [13]. In some cases, they can be doped to other nanoparticles while using as lubricant additives. Some of the examples of rare earth compound includes $Y_2O_3$, $LaF_3$, $CeO_2$, $La(OH)_3$, $CeBO_3$ etc.

Among those, some compounds were more popular than others. Metal oxides, metals, and sulfides made up the majority of nano-lubricants which is almost 65% [14] Table 2 shows the different types of nanoparticles and their statistics.

**Table 2:** Types of nanoparticles.

| Types | Total in percentage (%) |
|---|---|
| Metal Oxide | 26 |
| Metal | 23 |
| Sulfide | 16 |
| Nanocomposites | 6 |
| Rare Earth Compounds | 7 |
| Carbon | 7 |
| Other | 15 |
| | Total = 100 |

Moreover, Considering the morphology, nanoparticles can currently be classified into five categories: Spherical, Granular, Onion, Sheet, Nanotube [13]. The most common morphology of nanoparticles is spherical, followed by granular, sheet, onion, and nanotube. Nanoparticle morphology should also be taken into consideration when selecting a type of nanoparticle for use. Statistics of the morphology of nanoparticles are shown in Table 3.

**Table 3:** Morphology of nanoparticles.

| Morphology | Total in percentage (%) |
|---|---|
| Spherical | 57 |
| Granular | 12 |
| Onion | 9 |
| Sheet | 14 |
| Nanotube | 8 |
| | Total = 100 |

### 2.3.2 Lubrication Mechanisms

Lubrication is very important to overcome and reduce friction between two interacting surfaces or moving parts in relative motion [13]. Nanoparticles can penetrate the small gaps

between two surfaces due to their extremely small size [15]. A variety of mechanisms have been proposed to explain the lubrication mechanism of nanoparticles; the rolling effect [16], protective film [17], mending effect [18] and polishing effect [19] are all examples of nanoparticle lubrication mechanisms that have already been identified. These are all shown in Figure 1 [15]. These mechanisms can be mainly classified into two groups [16]. The first one is direct lubrication enhancement of nanoparticles (ball bearing effect/protective film formation), and the second one is surface enhancement (polishing/mending) of nanoparticles.

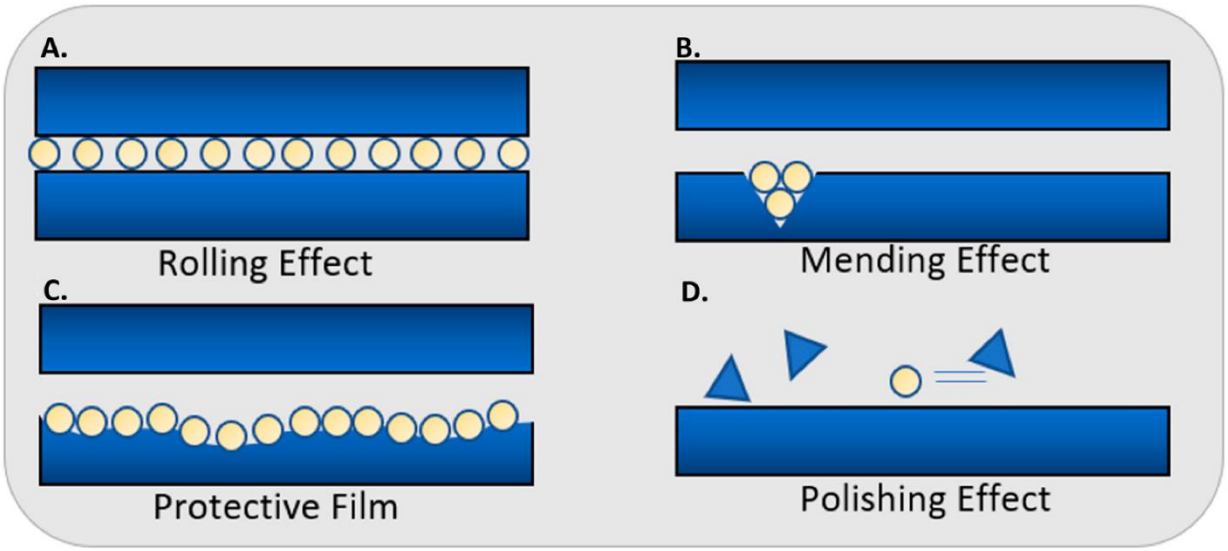


**Figure 1:** Lubrication mechanism of nanoparticles [15].

In rolling effect mechanism, nanoparticles (normally spherical or quasi spherical) suspended in lubricating oil play the role of ball bearings between the friction surfaces. The rolling effect makes the nanoparticles roll in between two surfaces and converts the sliding friction to the combination of sliding and rolling friction.

In addition, they also make a protective film or amorphous layer to some extent by coating the rough friction surfaces to enhance the protection of the surface. This protective film reduces the real area of contact which can significantly reduce the friction.

The nanoparticles deposit and accumulate on the rubbing surface and compensate for the loss of mass, which is known as mending effect [17]. It allows nanoparticles to fill out any pores or scars that can be found on the surface of the specimens being tested.

And the roughness of the lubricating surface is reduced by nanoparticle-assisted abrasion, which is known as a polishing effect [18]. In this mechanism, the nanoparticles polish the rubbing surface. The polishing effect helps to remove any asperities that can be found on the surface to reduce the friction and to smoothen out surface of the material. This effect is also known as smoothing effect.

### 2.3.3 Montmorillonite (MMT) Nanoclay as Lubricant Additive

Nowadays, a great variety of nanoclays are found commercially and phyllosilicate are one of the main categories among them. Montmorillonite (MMT) is a naturally occurring phyllosilicate material with a layered structure that has been widely used as a reinforcement for composite materials [19], [20]. Being environmentally friendly, naturally occurring, and economical, this Montmorillonite (MMT), a clay nanoparticle, has been proposed as lubricant additives for improving the tribological performance of lubricants [21]. MMT has a sandwich structure, wherein the upper and lower layers are silicon–oxygen tetrahedrons and the middle layer is aluminum–oxygen octahedron [22]. Moreover, exchangeable cations, such as $Na^+$, $Mg^+$, and $Al^+$, exist between the layers. Due to its unique characteristics of having a nanoscale layered structure and exchangeable cations, MMT can be easily modified and used for various applications [23-25]. Though the application of MMT for improving the tribological properties of polymer matrices has been well proved by many researchers [26, 27] their use as lubricant additives has not been studied in depth so far, to the best of the authors knowledge.

**Figure 2:** Montmorillonite nanoclay.

### 2.4 Potential Applications of Vegetable Oil Based Nano-lubricants

Vegetable oil-based nano-lubricants can be used in a wide range of applications. In the long term, fuel consumption and environmental pollution will be significantly reduced in automobile applications because of these unrivaled performance levels of vegetable oil-based nano-lubricants. The unique properties of nano-lubricants in terms of friction reduction and wear resistance serve as a steppingstone in the field of tribology and lubrication as well. This means that they can be used in metal cutting and other places where friction and wear need to be reduced. Their oxidation characteristics as well as their exposure to high temperatures are the main impediments to their use. The vegetable oils can be oxidized easily due to their unsaturated double bonds. As these oils tend to oxidize, they should be kept in closed systems.

# CHAPTER III

# METHODOLOGY

## 3.1 Nano-lubricants Formulation

The nanolubricants need to be prepared to perform the tribological and rheological tests. The formulation of nanolubricants is basically a two-step process. To prepare the nanolubricants and measure the weight of the block specimens being tested, a Mettler Toledo XS205DU electronic balance (Mettler-Toledo LLC, Columbus, OH, USA), as shown in Figure 3, was used. The accuracy of this device is 0.01 mg. A total of three weight measurements per block was measured before and after each test. After preparing the nanolubricants, they need to be placed in an ultrasonic mixer for the uniform dispersion of nanolubricants.

Nanolubricants were formulated using Equation (1),

$$wt.\%\ of\ nanoparticle = \frac{mass\ of\ nanoparticle}{Total\ mass\ of\ nanolubricant} * 100\% \quad (1)$$

Table 4 provides an overview of the lubricant's and nanoparticle's key properties.

**Table 4:** Material properties.

| Material | Properties |
|---|---|
| Lubricant | |
| Sunflower Oil | Density (40 °C): 0.92 g/cm$^3$<br>Viscosity (40 °C): 35 mPas |
| Peanut Oil | Density (40 °C): 0.92 g/cm$^3$<br>Viscosity (40 °C): 40 mPas |
| Corn Oil | Density (40 °C): 0.92 g/cm$^3$<br>Viscosity (40 °C): 32.53 mPas |
| Nanoparticles | |
| MMT (Montmorillonite) | Chemical Formula: $(Na, Ca)_{0.33}$ $(Al\ Mg)_2$ $(Si_4O_{10})$ $(OH)_2$. $nH_2O$ (Repeating unit) Density: 2.35 g/cm$^3$, Purity: 99%, Particle Size: 0.96 nm, Crystal System: Monoclinic, Hardness: 1-2 on Mohs scale |
| Specimens | |
| Blocks | AISI 304 steel, dimensions: 14 × 6.35 × 6.35 mm, hardness: 128 HRB |
| Rings | AISI 52100 steel, d = 40 mm, hardness: 60 HRC |

In a 20 ml flask, nanoparticles were added to vegetable lubricants (sunflower, peanut, and corn) at 0.5-3.0 wt.% concentrations. The overall working procedure is described below:

- At first, the electronic balance needs to be turned on by pressing the button as marked in Figure 3 and the weight should be set on 0.


**Figure 3:** Mettler Toledo XS205DU electronic balance.

- Then, the weight of an empty vial needs to be measured and the weight needs to be calibrated to 0 while the vial is placed on the balance.
- After that, using a spatula, MMT nanoparticles need to be placed on the vial according to the required concentration.
- Finally, the oil needs to be poured on it until the total weight is 15g.

Table 5 show the concentration used to prepare the different nano-lubricants.

**Table 5:** Preparation of nanolubricants.

| wt.% | Lubricant wt. (g) | MMT wt. (g) | Total wt. (g) |
|---|---|---|---|
| 0.50% | 14.9472 | 0.075 | 15.0222 |
| 1.00% | 14.8664 | 0.150 | 15.0164 |
| 1.50% | 14.8004 | 0.225 | 15.0254 |
| 2.00% | 14.7173 | 0.300 | 15.0173 |
| 2.50% | 14.6543 | 0.375 | 15.0293 |
| 3.00% | 14.5660 | 0.450 | 15.0160 |

Before testing, the nano-lubricants were mixed by ultrasonication to provide the best results by using a 120-Watt Fisherbrand$^{TM}$ Model dismembrator (Thermo Fisher Scientific Inc., Waltham, MA, USA), as shown in Figure 4a, at a frequency of 20KHz. The ultrasonication procedure is given below:

- At first, the probe of the dismembrator needs to be cleaned properly by ethanol and the vial needs to be placed on properly.
- The probe needs to be submerged on the nanolubricants.
- After that, the ultrasonic mixer needs to be turned on by pressing the “ON” button as marked in Figure 4a.
- Then the ultrasonication process needs to be started by pressing the “START” button, as shown in Figure 4a. Ultrasonication was done for 6 minutes (3 seconds on and 3 seconds off).
- After that, the ultrasonic mixer needs to be turned off by pressing the “OFF” button as marked in Figure 4a and the probe must be cleaned again by ethanol.
- Nanolubricants after ultrasonication are shown in Figure 4b.

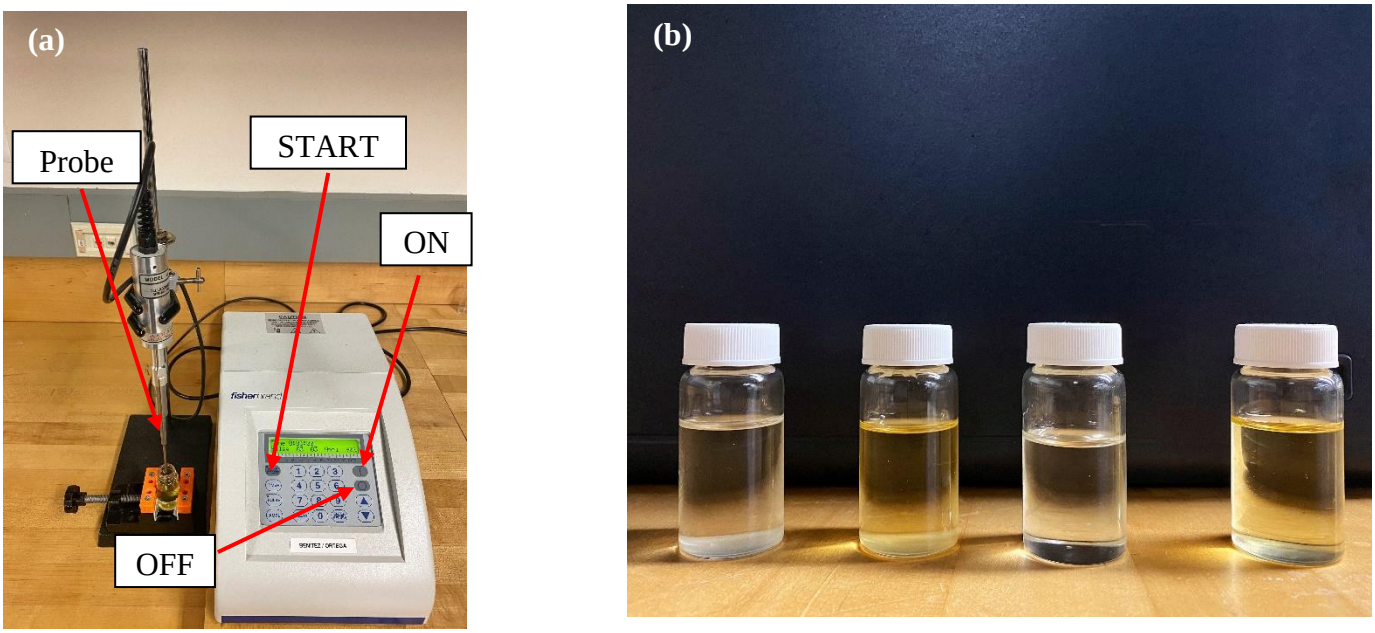


**Figure 4:** (a) 120-Watt Fisherbrand$^{TM}$ Model Ultrasonic mixer, and (b) Nano-lubricants after ultrasonication.

### 3.2 X-Ray Diffraction (XRD)

XRD is a non-destructive test method which is used to determine the structure of crystalline materials. XRD analysis is used to identify the crystalline phases present in a material to further reveal chemical composition Identification of phases is achieved by comparison of the acquired data to that in reference structures. Minerals, polymers, corrosion products, and unknown materials are all evaluated using it. It is highly used for evaluating minerals, polymers, corrosion products, and unknown materials. In most cases, the samples analyzed by powder diffraction using samples prepared as powders. The characteristics used to determine in XRD are

structural properties, lattice parameters, strain grain size, epitaxy phase composition, preferred orientation, measure thickness of thin films and multi-layers, atomic arrangement etc.

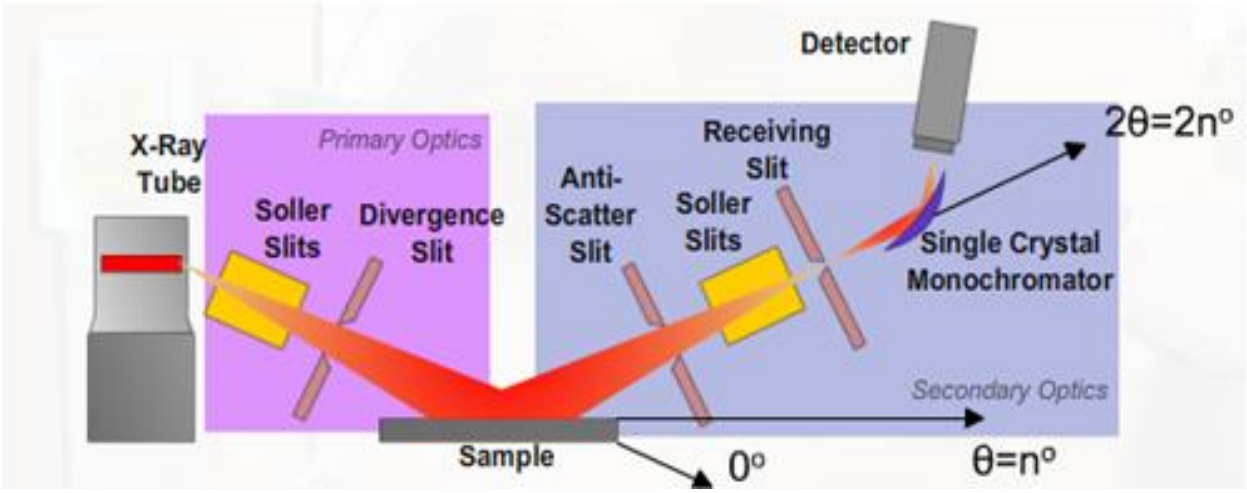


**Figure 5:** Schematic diagram of XRD analysis [23].

In our experiment, the MMT nanoparticles were analyzed using an X-ray diffractometer (XRD). Powder XRD patterns of the nanoparticles were recorded using a Rigaku Miniflex Benchtop diffractometer (XRD) with Cu Kα1 radiation ($\lambda$ = 0.15406 nm) which is shown in Figure 6a. The XRD data were collected using a scanning mode of $2\theta$, ranging from 10° to 70°, with a scanning step size of 0.01° and a count time 2s/step. At first, a coolflow refrigerator as shown in Figure 6b was turned on and needed to wait until the temperature of the XRD machine reached at 18 degrees or below. After that, the Miniflex devicee was turned on and the sample was carefully placed. After each run, it was needed at least 20 minutes to cool down the machine.


**Figure 6:** (a) Rigaku miniflex benchtop, and (b) coolflow refrigerated recirculator.

### 3.3 Thermogravimetric Analysis

In Thermogravimetric analysis (TGA), mass is continuously measured while the temperature of a sample is changed over time. In thermogravimetric analysis, mass, temperature, and time are regarded fundamental parameters, from which numerous additional measurements can be determined. A thermogravimetric analyzer includes precision balance carrying sample pan located inside a furnace. The temperature is generally increased at constant rate or different rate depending on the applications to incur a thermal reaction. The thermal reaction may occur under a variety of atmosphere such as: air, vacuum inert gas, gases, corrosive gases, carburizing gases, vapors of liquids as well as a variety of pressures. It is necessary to use the thermogravimetric data in order to create a plot showing the change in mass or percentage of initial mass as a function of time or temperature on the y axis. It is called TGA curve. The first derivative of the TGA curve is called the DTG curve.

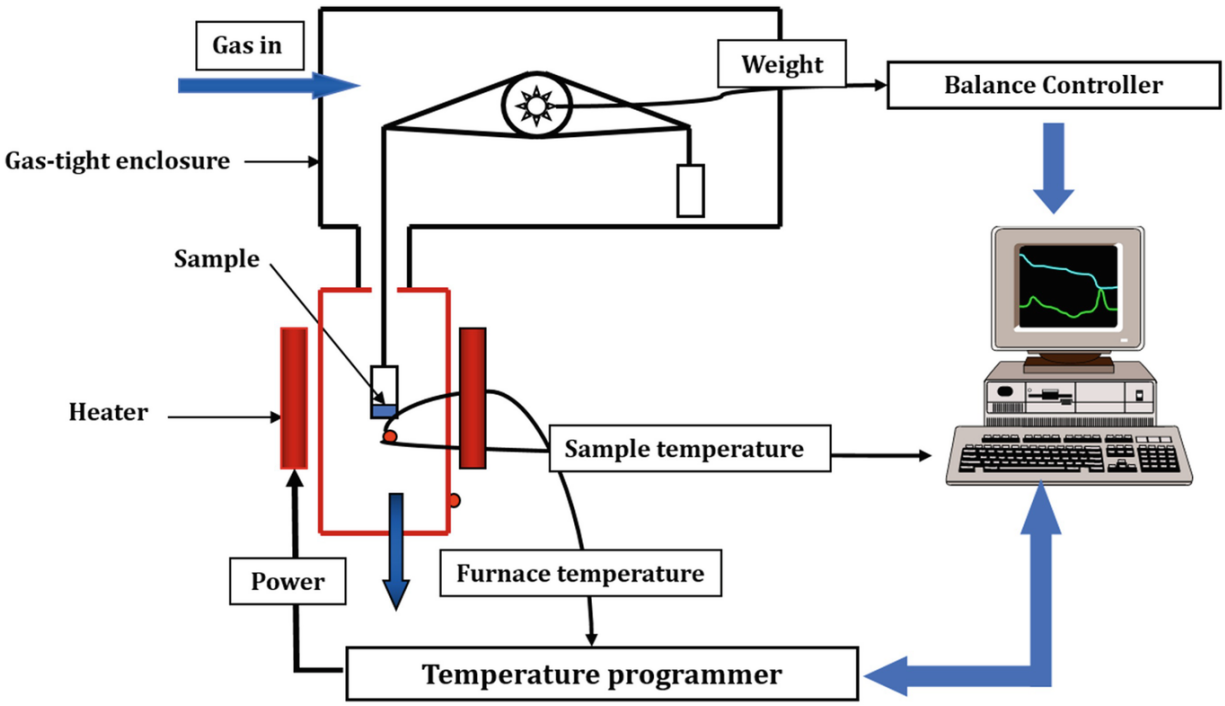


**Figure 7:** Schematic diagram of thermogravimetric analysis (TGA) [24].

In our experiment, the thermal properties were evaluated through thermogravimetric analysis (TGA) (TA Instruments, Q400) as shown in Figure 8. In order to perform the TGA analysis, the sample was heated from room temperature to 1000℃ under a nitrogen atmosphere, at a heating rate of $10Kmin^{-1}$. An open crucible, $Al_2O_3$ µl was used and the mass of the sample was 18.75mg.


**Figure 8:** Thermogravimetric analyzer.

### 3.4 Rheological Characterization

As depicted in Figure 9, a commercial rheometer HAAKE RS-150 RheoStress was used to measure the rheological properties of the nanolubricants in order to better understand their performance. A parallel plate and a spindle were used during experiment and the distance between two parallel plate was 0.5mm. MMT nanoparticles were dispersed in vegetable oils (Sunflower, peanut, and corn oils) and about 0.9mL sample was used to perform the test at a temperature of 23 ℃. The data was gathered at a shear rate range of 10 to 120 $s^{-1}$. The overall working procedure is described below:

- At first, the rheometer needs to be cleaned with acetone.
- Rheometer can’t be turned on until the pressure has stabilized in between 2.5 and 4.0 bar for 2.5 hours.

- The rheometer and temperature control need to be turned on (as marked in Figure 9).
- After turning on the computer, “Rheology Job Manager” software needs to be launched and then-

  Open new job ⟶ Flow curve: Ramp up only
- After opening the job editor window with rheometer model, a few parameters need to be selected:

  Spindle: PP35ER

  Temperature sensor: TC 501
- After that, some parameters need to be edited from the parameter window- shear rate range, time of the experiment.
- The amount of data points needs to be selected from the data acquisition tab.
- By opening the manual control window, the sample needs to be loaded (Sample needs to be touched on both sides of the parallel plate).
- After placing the sample carefully, it needs to be clicked on the “Go to gap” menu.
- After closing the manual control window, finally the experiment needs to be started (Three trials for each one) and the density of the sample needs to be put. Density of the sample can be calculated by using Equation 2,

$$Density\ of\ the\ sample = \frac{total\ weight\ of\ nanolubricant\ (g)}{(volume\ of\ lubricant + volume\ of\ MMT)(cm^3)} \quad (2)$$

  The value needs to be multiplied by 1000 to convert the density into kg/m$^3$.
- After the experiment, it needs to be clicked on the down arrow of the rheometer and rheometer needs to be cleaned again with acetone.

- Finally, rheometer and temperature control need to be turned off.


**Figure 9:** Commercial rheometer HAAKE RS-150 RheoStress.

Viscosity of nanolubricants depend on some factors such as temperature, shear rate, particle size, volume concentration. The nanolubricants can exhibit either shear thinning or shear thickening characteristics. If the viscosity decreases with increasing shear rate, it's called shear thinning and if it exhibits the opposite characteristics, then it's called shear thickening.

### 3.5 Tribological Characterization

To perform the tribological test, at first, block specimens were prepared by cutting an AISI 304 steel square bar into blocks of required sizes shown in Figure 10a. To cut the blocks according to the required sizes, a DAKE JOHNSON heavy-duty bandsaw machine (Model-JH10, Grand Haven, Michigan) was used, as shown in Figure 10b.

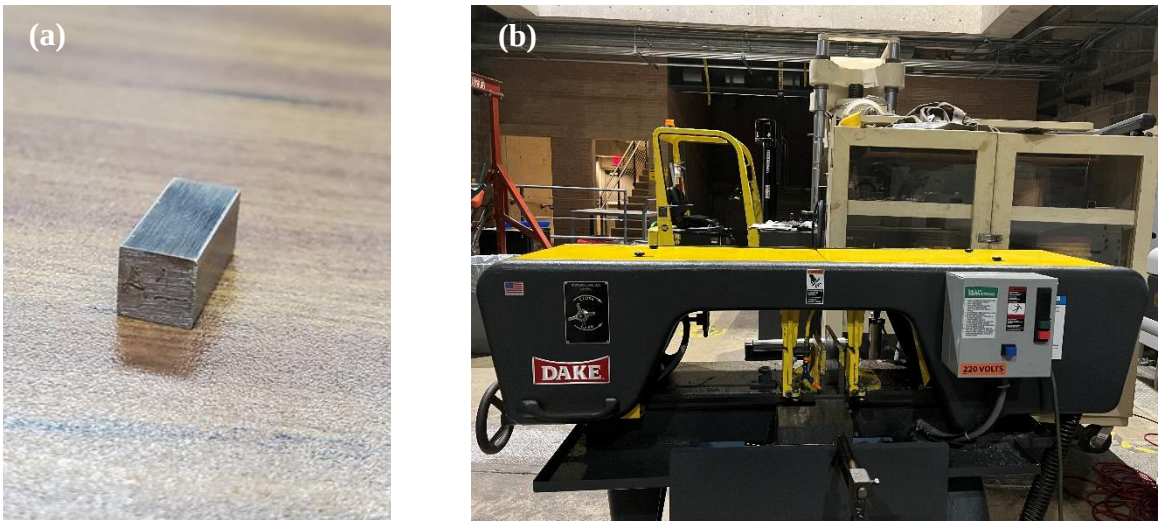


**Figure 10:** (a) AISI 304 steel square raw block, and (b) heavy duty horizontal bandsaw machine.

After that, the blocks were placed into the NANO 1200T Grinder Polisher (Pace Technologies), shown in Figure 11.


**Figure 11:** Nano 1200T Grinder Polisher.

The main purpose of this machine was to sand down the blocks to reduce the surface roughness and ensure similar kind of surface textures for all the blocks. The overall working procedure of this machine is given below:

- At first, the machine needs to be turned on by pressing the "ON/OFF" button, as marked in Figure 12a. This button is located at the back of the machine.
- After that, the grit paper needs to be attached on the top surface of the machine, as shown in Figure 12b.

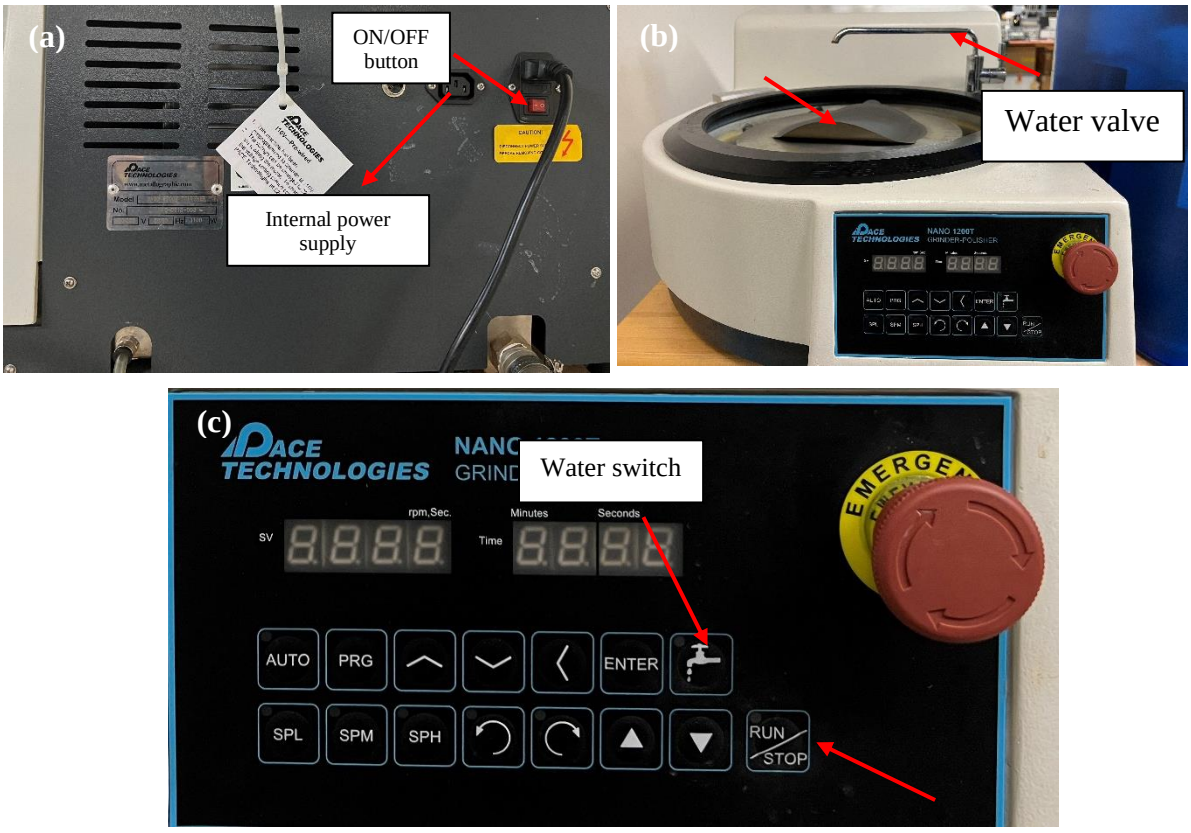


**Figure 12:** Nano 1200T Grinder Polisher showing: (a) back view, (b) front view, and (c) control panel.

- After attaching the grit paper properly, the "Water switch", as marked in Figure

12c, needs to be turned on. The flow of water can be adjusted by using the “Water valve”, as shown in Figure 12b.

- In this process, grinding or polishing needs to be done by hand. After setting everything manually, the “Run/Stop” button needs to be turned on to start the operation, as shown in Figure 12c.
- As stainless steels have high concentrations of chromium (>12%) and are generally relatively soft as compared to heat-treated steels, the grinding/polishing operations needs to be done by using 240, 360, and 600-grit paper sequentially.
- When necessary, the abrasive paper should be replaced with a newer paper.
- After preparing the blocks, the machine needs to be turned off by pressing the “ON/OFF” button, as shown in Figure 12a.

After polishing, blocks contained dirt, grease which could affect the weight measurements. To solve this problem, the blocks were required further cleaning. After preparing the block specimens, they were placed into the ultrasonic cleaner, as shown in Figure 13.

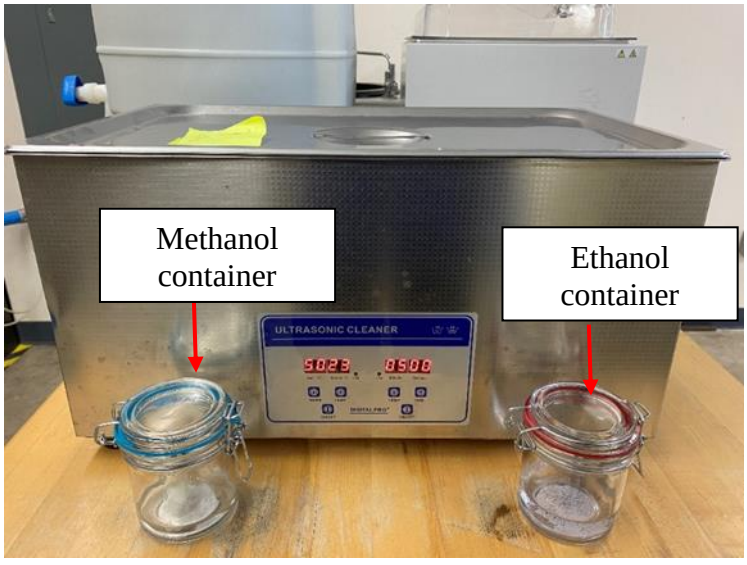


**Figure 13:** Ultrasonic cleaner.

This is basically a 2-step cleaning process. The overall working procedure is given below:

- At first, the ultrasonic cleaner machine needs to be turned on by pressing the "ON/OFF' button located at the back of the ultrasonic cleaner.
- After that, the blocks were introduced in a methanol container for 5 minutes, as marked in Figure 13.
- Then, the blocks were placed in a container of acetone for another, 5 minutes as shown in Figure 13.
- Finally, it was needed to keep the blocks in a closed chamber for at least 12 hours.

After finishing all these above operations, a custom-made block on ring tribotester was used to evaluate the sliding wear and friction behavior of the nano-lubricants. This test setup typically involved a block loaded against a rotating shaft or ring. A load of 266 N was used to perform the sliding wear and friction tests. This test was done at a temperature of 23 ℃, at 173 rpm, and the total time required to complete the test was about 20 minutes. A block density of 8 $g/cm^3$ (corresponding to the stainless steel) was used to convert the wear mass into volumetric loss. Figure 14 shows the tribotester while experimentation of nano-lubricants is being performed.

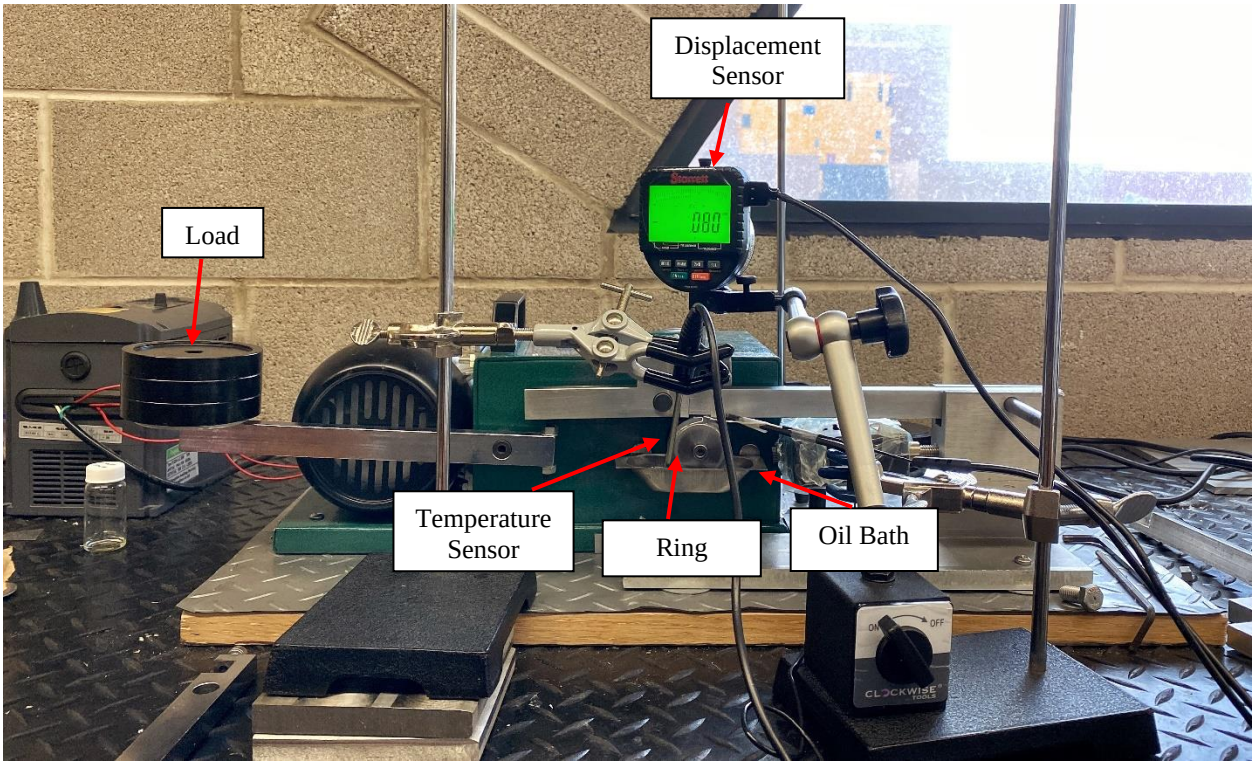


**Figure 14:** Custom-made block on ring tribotester.

The overall working procedure is given below:

- At first, control panel needs to be turned on by pressing the “ON/OFF” button, as marked in Figure 15a and the speed needs to be set at 173 rpm.
- A variable frequency drive (VFD) controller inverter is required to regulate the frequency. The frequency adjuster knob needs to be used to adjust the frequency as marked in Figure 15b.


**Figure 15:** (a) Control panel, and (b) VFD controller inverter.

- After that, the cylindrical ring needs to be placed as shown in Figure 14. For each of the nanolubricants, different set of rings should be used.
- The surface of the ring needs be polished using 360 and 600 grit papers and after polishing, the ring needs to be cleaned by acetone to remove any dirt.
- Then, the oil bath chamber needs to be cleaned properly and placed below the ring, as shown in Figure 14.
- After placing the oil bath chamber, lubricant needs to be put into it and the cylindrical ring should be rotated manually at least 3 times to lubricate it properly.
- After that, the block that was prepared earlier, needs to be adjusted to the short arm by screw.
- Then the short arm needs to be placed horizontally (as shown in Figure 14) by using a mercury surface level tool.

- A constant load of 266 N needs to be applied to the left end of the lower arm.
- After that, the displacement sensor needs to be mounted on the top of the arm, just above the fixed block position and the temperature sensor needs to be submerged partially in the oil bath chamber, as depicted in Figure 14.
- Vernier LABQUEST data logger needs to be turned on and connected to a power source, as shown in Figure 16a.
- Force sensor (Channel 1) and temperature sensor (Channel 2) need to be connected to the Vernier LABQUEST data logger, as shown in Figure 16b.

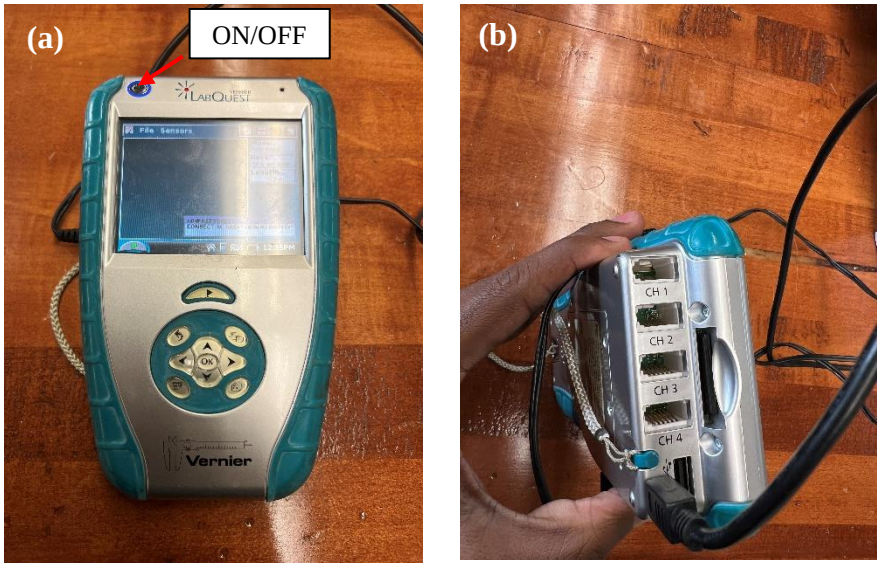


**Figure 16:** Vernier LABQUEST data logger: (a) front view, and (b**)** power cable and channels.

- After opening the "Logger lite" software, these steps need to be followed:

  Go to Experiment/Data Collection.

- From date collection, the data needs to be set as:

  Time duration-1240 sec.

  Sampling rate-10/sec

- After that, force sensor needs to be fixed in channel 1 and the temperature sensor in channel 2 by following these steps:

  Go to Experiment/Set up sensor.

- Then, the displacement sensor needs to be turned on by using the power button.
- After that, “Electronic Measuring System” software needs to be opened and the initial displacement value needs to be set to zero.
- After each run, the data needs to be saved as both csv and text format by following these steps:

  Go to File/Export data.

## 3.6 Surface Characterization

Surface characterization was performed by measuring average roughness of the wear scars of the worn-down specimens and by analyzing the morphology of the worn surfaces as well.

### 3.6.1 Roughness

As depicted in Figure 17, a MarSurf M300 C surface profilometer was used to analyze the surface roughness of the wear scars of the worn-down specimens corresponding to the best concentration. This device could measure up to 350 μm.

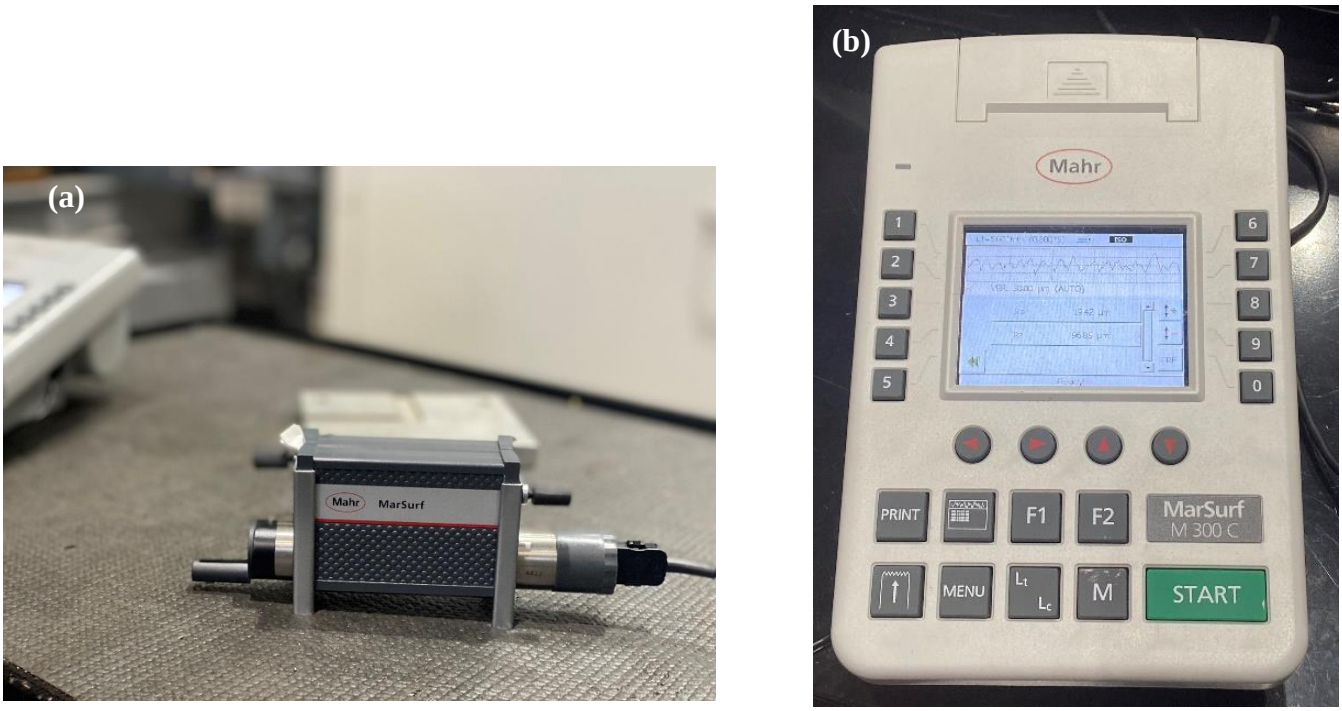


**Figure 17:** MarSurf M300 C profilometer: (a) profilometer, and (b) thermal printer.

After finishing the tribological tests, the most compatible blocks due to the volumetric wear were chosen carefully. The roughness of the most compatible blocks was measured by the surface profilometer. The overall working procedure is given below:

- At first, the power cable needs to be plugged in as marked in Figure 18a.
- Then the surface profilometer needs to be turned on by pressing the “START” button as showed in Figure 18b.
- After turning the machine on, the probe of the profilometer needs to be calibrated as:

Rz = 9.3 μm = Maximum roughness.

Ra = 2.4 μm = Average roughness.

- Once the calibration has been done, the block needs to be placed under the probe as marked in Figure 18c to find the roughness. The roughness test was done on the blocks lubricated with base oil and the most compatible blocks.


**Figure 18:** MarSurf M300 C profilometer indicating: (a) power cable, (b) "START" button, and (c) probe.

- For each block, the roughness was measured three times on the wear and three times on the untested section. Finally, three values were averaged to get the perfect result.

### 3.6.2 Scanning Electron Microscope (SEM)

The morphology of the MMT nanoparticles and the worn surfaces of the block specimens were studied using a scanning electron microscope (SEM). Preparation of the samples for the SEM is a very important procedure in order to conduct the SEM characterization technique correctly. One reason why SEM is a good characterization technique is that the amount of sample needed is very small.

The first step on preparing the sample is to place a carbon tape, where the sample will be pasted on to, in order to stick to the sample holder. Carbon tape plays an important role on the preparation of the sample since it is a conductive material. Once the sample has been prepared,

the following steps are required to analyze the sample. First the vent is to be pressed to let air into the vacuum chamber. Once venting is completed, the sample chamber door can be open, and the sample can be fixed into the sample holder.

Once the door is open, the sample is loaded. Once the sample is loaded into the sample holder, screws that hold the sample in place is to be tightened. Then, the sample holder is proceeded to slide into the sample chamber and closed the chamber door by pushing it back. After making sure that the sample chamber door is closed, the vacuum is turned on. The vacuum is necessary to remove air molecules which allows electrons to have a clear path to the sample. Once the internal pressure is about $10^{-6}$ torr and the ETC gun is ready to be turn on, the desired sample can be analyzed.

After that, the command window is opened and set the sample holder to a safe distance (green line) from the detector sensors. Then a detector will be chosen, the SE is the most commonly used and will work on most samples. Finally, an accelerating voltage is applied. Then, the focus knob left is turned on and right to center the image. Once the image is sharp the focus knob is let go of X and start moving the sample around with the joystick to find any regions of interest. Also, the magnification of images can be increased or decreased using the magnification knob. To produce sharper images, it's necessary to focus at a magnification greater than that of imaging. Images that are streaked or smear are caused due to the beam spot not being circular. To correct this, turn the stigmation knob until a clear image is obtained. Also, if the image wobbles/oscillates in the x and y axes, the wobble adjuster is used to bring optics into alignment.

The final adjustment that can be made to the sample is the scan rate. The scan rate is the speed at which the beam moves across the sample surface. Image quality will increase as the

scan rate increases but will take longer to scan the sample. Once the set scan rate produces a proper image, the image will freeze by pressing the freeze button. This would allow acquiring a photograph of the image being analyzed.

When finished imaging, the beam is turned off and vented the vacuum chamber. When it's safe to do so remove the sample from the sample chamber, the chamber door is closed, and made sure to turn off the SEM program.

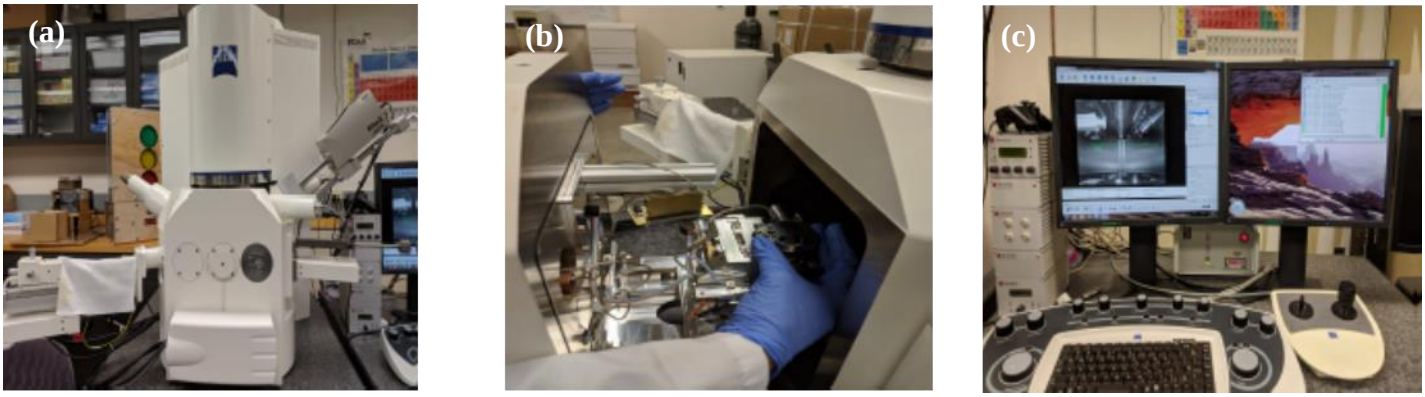


**Figure 19:** Outer structure of an SEM: (a) front view, (b) inside view of SEM, and (c) display/ data output device.

Scanning electron microscope, SEM (Carl Zeiss, SigmaVP) was used to observe the morphology of MMT nanoparticles and wear scars of the blocks. As the MMT nanoparticle is conductive, no sputtering with gold-palladium before examination were needed. Different SEM images at the same magnification were used to determine the average diameter. The images were processed by ImageJ software. At least 20 measurements were taken from each image in order to have 100 measurements in total. The mean value and standard deviation were determined with the help of MINITAB® software.

### 3.7 Tapping Torque Tests

A custom-made tapping torque tester [25] was used to perform the tapping torque tests. This test was done to determine the torque acting on the aluminum specimens in order to study the nano-lubricants behavior in real-world applications. The overall procedure is given below:

- At first, aluminum 6061 specimen needs be cut from an aluminum bar at a length of 38.1 mm (1.5 inch) using a heavy-duty horizontal bandsaw machine as shown in Figure 10b to achieve the desired length.
- After that, both side of the aluminum specimen needs to be faced properly as shown in Figure 20 by using a lathe machine.

**Figure 20:** Aluminum specimen.

- A Grizzly milling machine G0796, as shown in Figure 21, is required to perform the tapping torque tests. The tapping torque tester needs to be placed on the bed of the milling machine properly.


**Figure 21:** Grizzly milling machine G0796.

- The tapping torque tester needs to be fixed properly and the specimen needs to be adjusted to the specimen holder by using a screw before every run. Figure 22 shows a custom-made tapping torque tester mounted on a Grizzly milling machine.

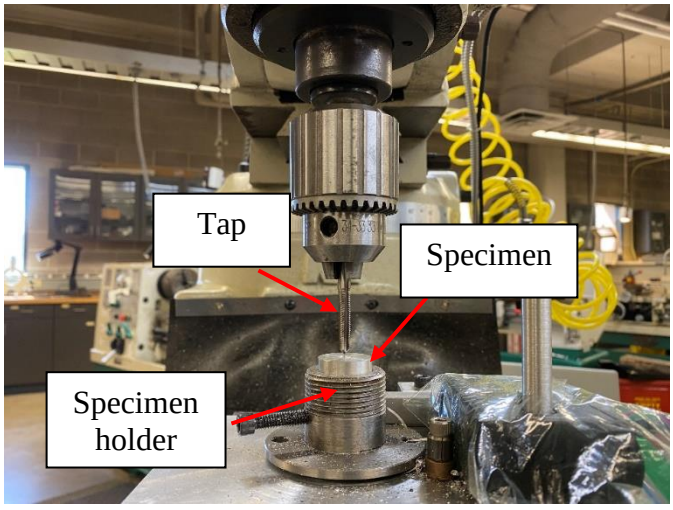


**Figure 22:** Custom-made tapping torque tester.

- After adjusting the specimen, it needs to be centered properly.
- Then the specimen needs to be drilled up to 33.02 mm (1.3 inch) using a drill bit. This drilling operation should be performed at a high speed. The distance between the high and low levers should be the maximum while setting the high speed.
- After the drilling operation, the tap needs to be set properly, as shown in Figure 22. Taps of size M6 x1.00 mm was used during the experiment, and a depth of 31.75 mm (1.25 inch) was reached.
- After that, LABQUEST Vernier data logger needs to be turned on and the force sensor needs to be connected to the vernier.
- After opening the "Logger lite" software in the computer, some steps need to be followed as:

  Go to Experiment tab, then chose Data collection.
- From data collection, the time duration needs to be set as 20 seconds.
- After that, force sensor needs to be fixed in channel 1 by following these steps-

  Go to Experiment tab, then chose Set up sensor.
- The force direction needs to be reversed to obtain the positive value.
- Then, the speed of the milling machine needs to be fixed as 90 rpm. To set the speed, the distance between two levers needs to be minimized.
- A volume of 0.5mL needs to be used to lubricate the taps properly before running the test.
- During the test, it is important to remember to run the test to a depth of 31.75 mm (1.25 inch) while controlling the lever to the downward position.

- The speed needs to be changed in reverse direction which allows the tapper to come out automatically from the aluminum specimen.
- After each run, the data needs to be saved as csv and text format by following these steps:

    Go to File/Export Data.
- A total of six taps being used throughout this experimentation process. Each tapping process was repeated two times for each lubricant. At first, a tap was used for base oil and then another tap was used for each of the best performing nano-lubricants (Due to the volumetric wear).
- This same process was followed for each lubricant.

# CHAPTER IV

# RESULT AND DISCUSSION

## 4.1 Morphology (MMT SEM Analysis)

From Figures 23 (a) and (b), it could be noted that the MMT nanoparticles were found to be spherical in shape. From the Figure 23a, it could be observed that MMT nanoparticles exhibited a kind of uniform morphology, though not uniform everywhere. We could notice some spaces among layers where active materials were attached, and particle pulverization might be negligible. It can be observed that nanoclays are in the form of large and small aggregates [26]. The surface morphology of MMT nanoparticles exhibited a layered surface with some large flakes, which is a typical structure for MMT, and some pores could also be found. Moreover, the diameter of MMT nanoparticles might be in the micrometer range. From figure 23d, the inserted SEM image with high magnification demonstrated that the mastoid was constituted by number of fragments, like a “flower cluster”. The surface pictures of the montmorillonite clay sample used in this study are comparable to those found in the literature [27].

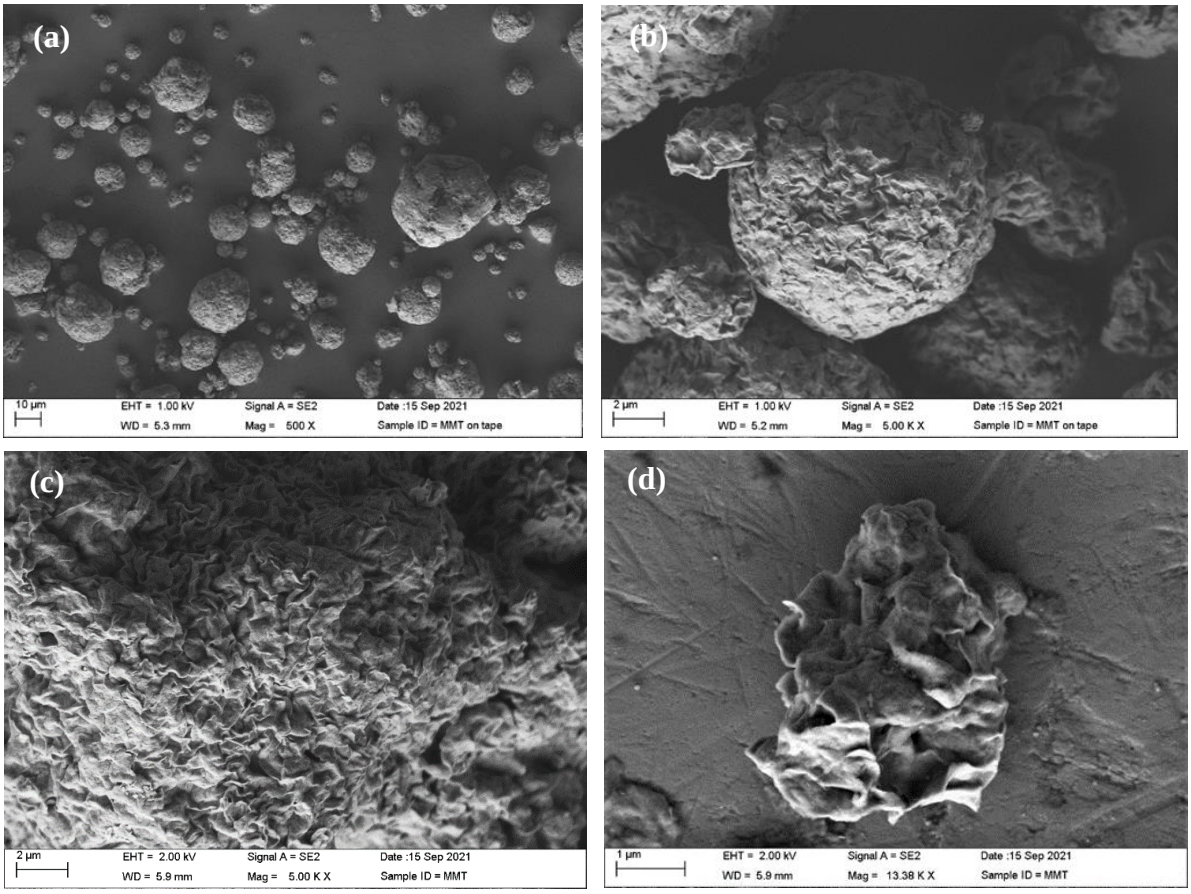


**Figure 23**: Morphology of MMT Nanoparticles under different magnification: (a) 500 X, (b) 5 KX, (c) 5 KX, and (d) 13.38 KX.

Figure 24 shows the normal distribution of MMT nanoparticles by which we could get an idea of the diameter of the MMT nanoparticles. The average diameter of the samples was found to be 7.57µm. Though most of the nanoparticles ranged in between 0-5µm, a few of them were significantly large in diameter compared to the others which could be a reason behind exhibiting a large average diameter. From the figure, it could be observed that almost 80% of the nanoparticles were less than 10µm, almost 18-19% of the nanoparticles ranged in between 10-

25µm and a few were above 30µm. More research in this area could bring idea about the size of the particles and their orientation.

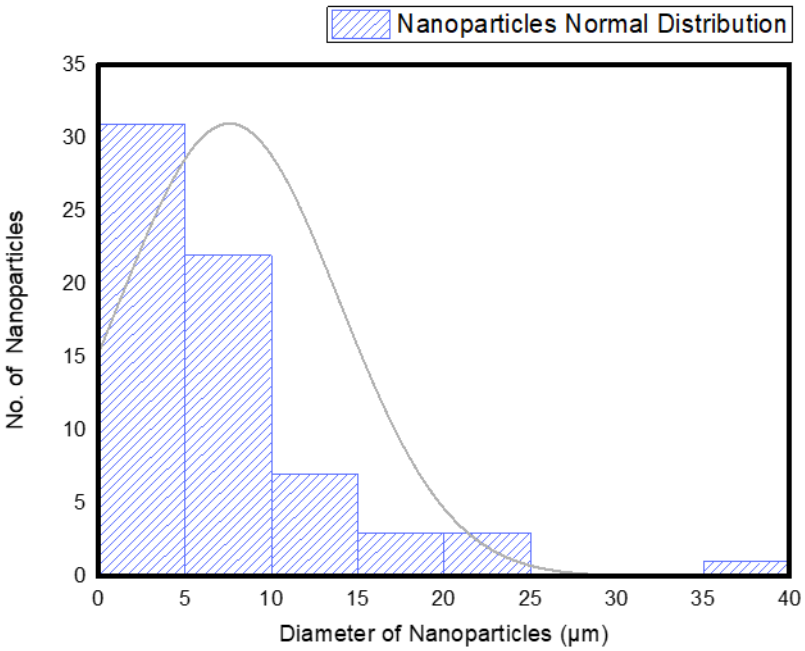


**Figure 24:** Normal Distribution of MMT Nanoparticles.

## 4.2 XRD Analysis:

From Figure 25, the XRD pattern of Montmorillonite nanoclay can be observed. The data collection parameters are: Source Co kα (1.789 Å), from 10 to 70 in 2θ, step size 0.01°, and count time 2s/step.

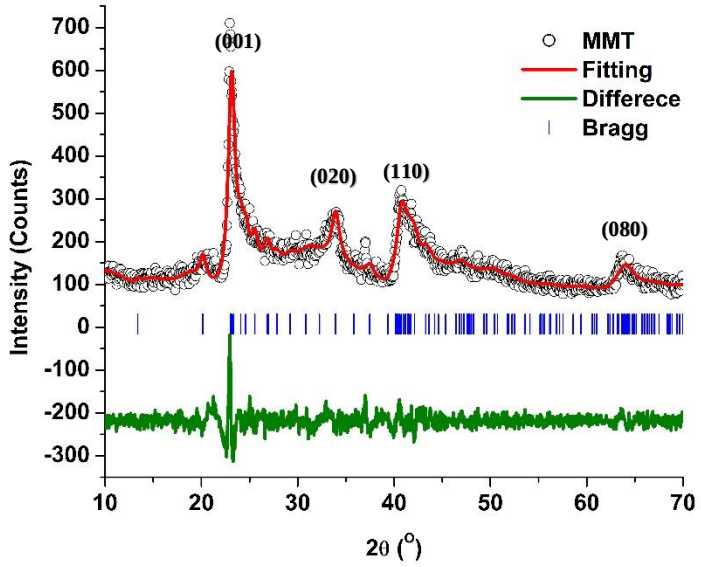


**Figure 25:** XRD analysis of MMT nanoparticles.

Figure 25 demonstrated the crystallographic parameter of MMT nanoclay. It can be determined by measuring the (001) peaks at around 2θ = 22.5° which indicated a diffraction peak and (080) peaks at 2θ = 64.5° which indicated the dioctahedral structure of MMT [27]. The diffraction peak at 2θ = 22.5° corresponded to basal spacing of 15.452 Å. The diffraction signals found at 34.5°, 41.6°, 64.5°. The pattern we found in our XRD analysis is quite similar to those found in the literature. The Montmorillonite peaks denoted 2:1 swelling clay and the other peaks seemed to be impurities.

Lattice parameter can be determined by using the LeBail fitting procedure as shown in Table 6.

**Table 6:** Lattice parameter for MMT nanoparticles.

| Sample | Space Group | a(Å) | b(Å) | c(Å) | α(°) | β(°) | γ(°) | χ2 |
|---|---|---|---|---|---|---|---|---|
| MMT | C2/m | 5.224(6) | 8.938(9) | 15.452(3) | 90 | 96.43 | 90 | 1.54 |

From Table 6, it can be observed that, length of unit cell, a= 5.224 Å, b= 8.938 Å, c= 15.452 Å and $\alpha = \gamma = 90°$, $\beta \neq 90°$, which indicated the monoclinic structure of Montmorillonite nanoclay.

## 4.3 Thermogravimetric Analysis:

The TGA analyses was carried out by using a NETZSCH TG 209F3 analyzer to determine the thermal stability of Montmorillonite (MMT) nanoclay. The powder sample of MMT was placed in a 85µl, open crucible. A constant heating rate of 10K/min was applied from 27°C to 1000°C within an open ceramic pan. The mass of the sample was 18.75mg and the whole process was done under a nitrogen atmosphere with a flow rate of 20ml/min.

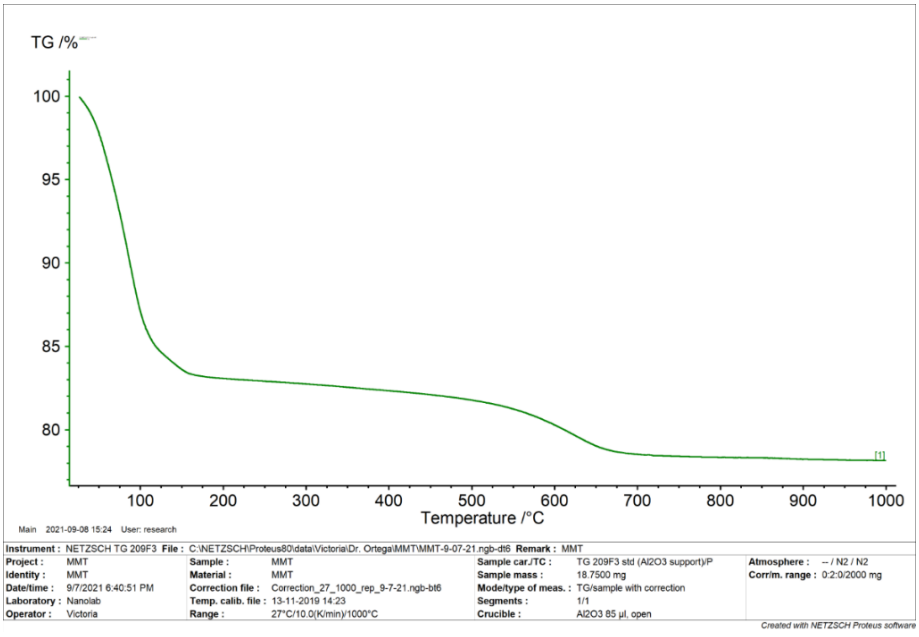


**Figure 26:** Thermogravimetric analysis curve of MMT nanoclay.

The TGA curve of MMT modified in a Nitrogen atmosphere is shown in Figure 26. The MMT nanoparticles lose about 22% of their total mass during the heating process (From room temperature to 1000°C). A sudden mass loss of about 17% was observed from room temperature to 150°C. The evaporation of the absorbed water on the surface of MMT may be the reason behind it. After that, there was no significant mass loss was observed up to 550°C. The mass loss remained quite unchanged in the range of 150°C to 550°C. A slight mass loss of 5% was observed from 550°C to 680°C because of the gradual loss of crystal water. Finally, a very negligible loss of mass was seen from 680°C to 1000°C.

## 4.4 Rheological Measurement Analysis:

As depicted in Figure 9, a commercial rheometer was used to study the characteristics of vegetable oils that had been modified with MMT nanoparticles. Various concentrations (0.01%-0.10%) of MMT nanoparticles were dispersed in base oil to see the effect in rheological behavior. Among three base oils, peanut oil exhibited the highest viscosity and all three oils seemed to keep a shear thinning behavior.

### 4.4.1 Rheological Analysis of Sunflower Oil Modified with MMT Nanoparticle:

In Figure 27, the rheological behavior of sunflower oil modified with MMT nanoparticle as additives can be observed. From the figure, base sunflower oil seemed to have the lowest viscosity at around 73 cP. Throughout the experiment, the viscosity didn't change that much for base sunflower oil. The addition of MMT nanoparticle increased the viscosity of the base oil and the highest viscosity was found to be at 0.10 wt.% concentration increasing the viscosity to about 87 cP. In all cases, viscosity decreased with the increase of shear rate; so, it seemed to keep a shear thinning behavior. Moreover, the addition of MMT nanoparticle increased the viscosity of

the nano-lubricants; the higher the concentration, the higher the viscosity. The nanoparticles in the lubricants were in the form of aggregates which made them less mobile. It could be the reason for exhibiting higher viscosity.

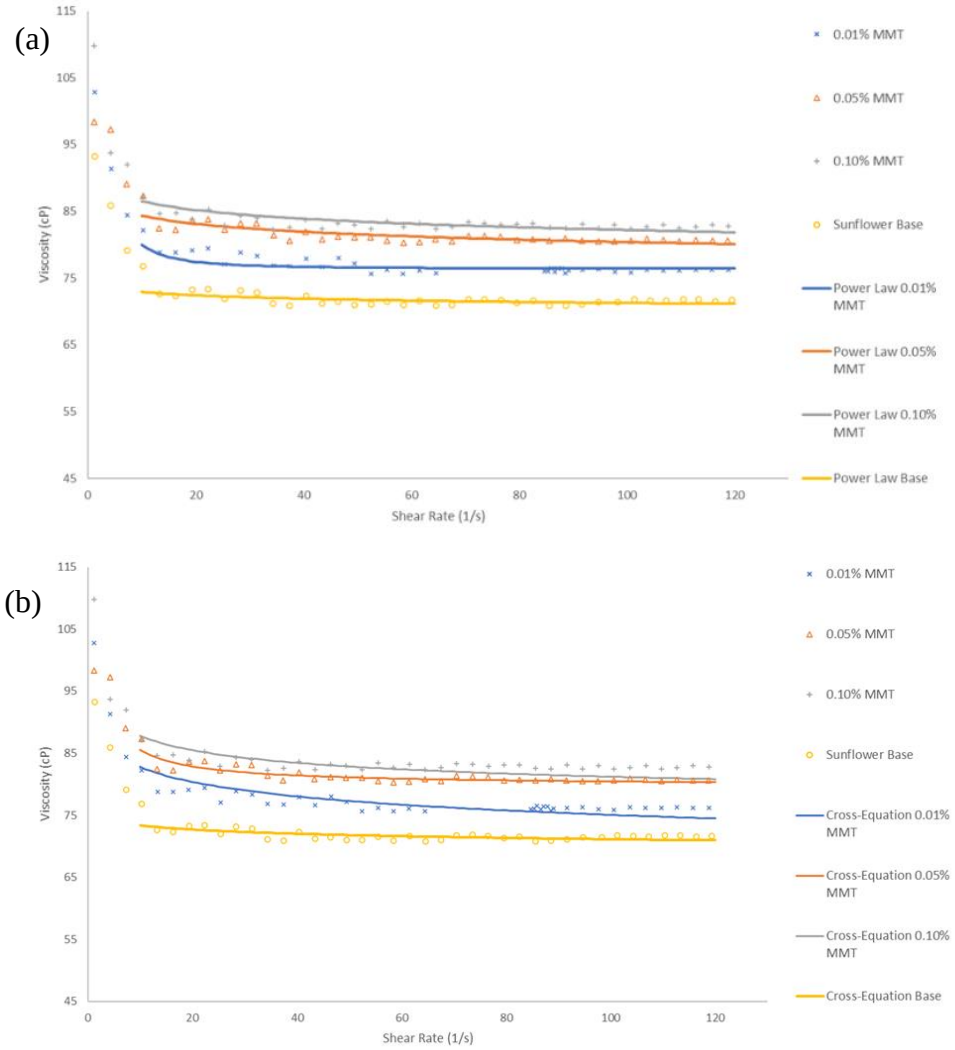


**Figure 27:** Viscosity vs shear rate for MMT dispersion in various weight fraction in Sunflower oil with (a) Power law model, and (b) Cross equation model.

### 4.4.2 Rheological Analysis of Peanut Oil Modified with MMT Nanoparticle:

Figure 28 shows the rheological behavior of peanut oil modified with MMT nanoparticles at different concentrations. Base peanut oil seemed to have the highest viscosity at around 86 cP. But initially 0.05 wt.% MMT modified peanut oil had the highest viscosity at around 90 cP. The addition of the MMT nanoparticles managed to lower the viscosity. The formation of less agglomerate could be the reason behind it because it increased the mobility of nanolubricants and decreased the viscosity. Like sunflower oil, the viscosity in all cases decreased with shear rate and kept a shear thinning effect. For peanut oil, the lowest viscosity was found to be at 0.10 wt.% concentration decreasing the viscosity to about 75 cP.

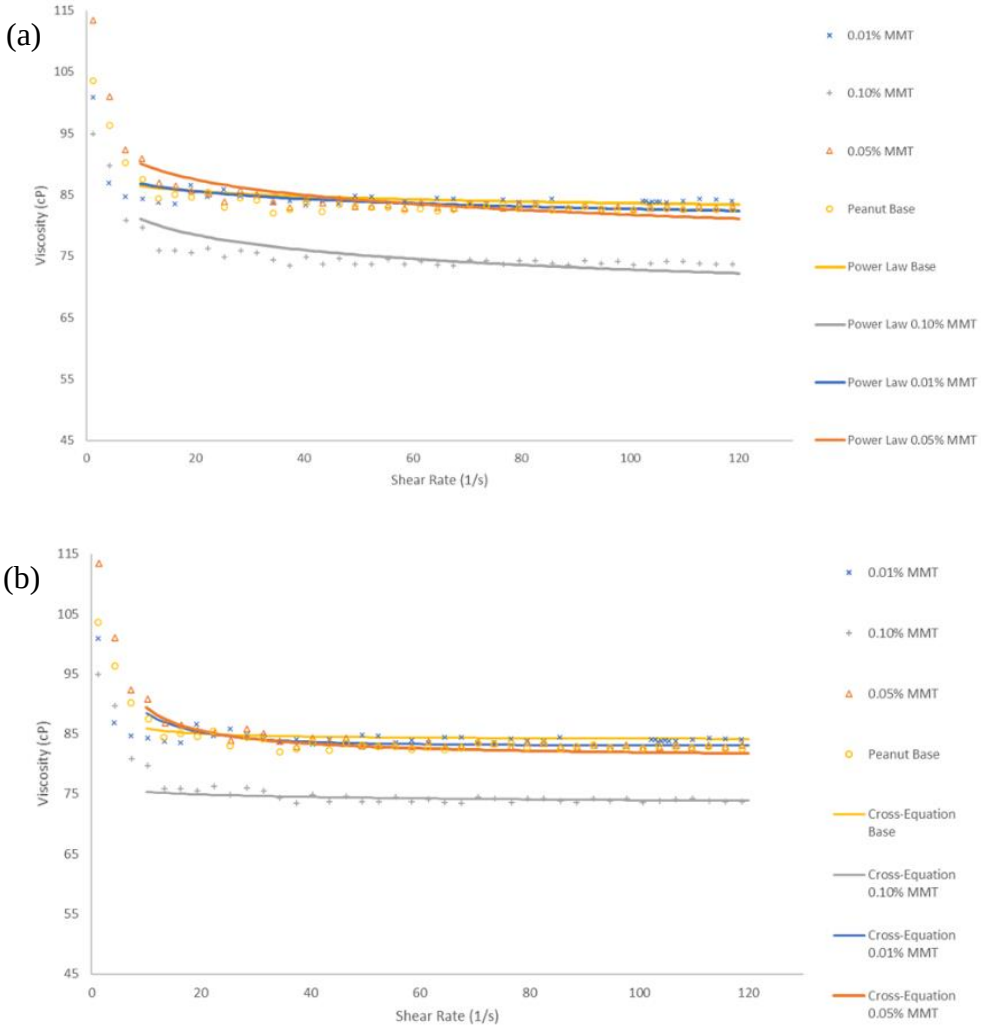


**Figure 28:** Viscosity versus shear rate for MMT dispersion in various weight fraction in Peanut oil with (a) Power law model, and (b) Cross equation model.

### 4.4.3 Rheological Analysis of Corn Oil Modified with MMT Nanoparticle:

In most part, base corn oil seemed to have the lowest viscosity ranging from 60 to 65 cP. Like sunflower oil, the addition of the MMT nanoparticles increased the viscosity of the base corn oil due to the formation of agglomeration. It created a shear thinning behavior to take effect as well because the viscosity decreased with shear rate. For corn oil, the highest viscosity was found to be at 0.10 wt.% concentration increasing the viscosity to about 73 cP.

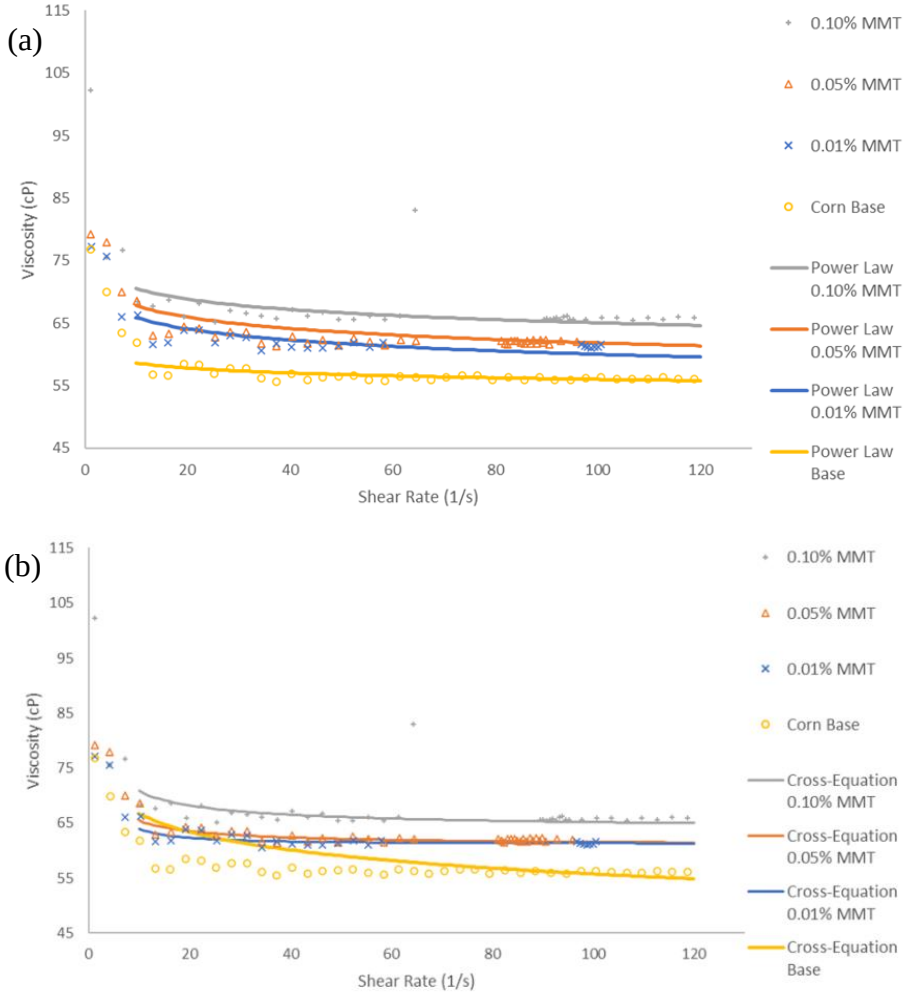


**Figure 29:** Effect of viscosity versus shear rate for MMT dispersion in various weight fraction in Corn oil with (a) Power law model, and (b) Cross equation model.

## 4.5 Rheology Model:

To characterize the relationship between shear stress and shear rate in non-Newtonian fluids, several mathematical models have been proposed. To improve the accuracy in predicting the viscosity of nanolubricants, Power and Cross equation models of rheological properties were used. Viscosities of the nanolubricants were measured at a shear rate range of 10 to 120 $s^{-1}$.

### 4.5.1 Power Model:

The viscosity term from the Newtonian model is replaced in the Power law model by a constant, K, referred to as the consistency index, which serves as the system's viscosity index. The relationship between viscosity and shear rate is best represented by the power law model as shown in Equation 3 and it is the most frequently applied model. The power law model can be expressed as-

$$\eta = K(\dot{\gamma})n - 1 \quad (3)$$

Here,

K= Consistency index.

n= Flow behavior index.

- It denotes the shear thinning characteristic of a fluid when n < 1; as shear rate increases, viscosity will decrease.
- It denotes a Newtonian fluid when *n* = 1, viscosity doesn't change with shear rate.

- It denotes the shear thickening characteristic of a fluid when $n > 1$; as shear rate increases, viscosity will increase.

### 4.5.2 Cross Model:

For non-Newtonian fluids, the Cross model was established based on the concept of pseudoplastic flow. Most non-Newtonian fluids have more complex behavior and are better described by the Cross model. The Cross Model is an empirical formula for fitting non-Newtonian data. The cross model is shown below in Equation 4:

$$\eta = \frac{\eta 0 - \eta \infty}{1 + (K\dot{\gamma})n} + \eta \infty \quad (4)$$

Here,

$\eta_0$= Zero shear viscosity.

$\eta_\infty$= Infinite shear viscosity.

K= Consistency index.

n= Flow behavior index.

Table 7 represents the regression parameter analysis of sunflower, peanut and corn oil modified with 0.05% MMT nanoparticle. The viscosity at this concentration situated at the middle for all three oils. That's why regression parameter analysis was done at 0.05% MMT modified base oils.

**Table 7:** Regression parameter analysis of sunflower, peanut and corn oil modified with 0.05% MMT nanoparticle.

| Lubricant | Model | Configuration | K | $R^2$ | n | η0 | η∞ | SSE |
|---|---|---|---|---|---|---|---|---|
| Sunflower | Power Law | Sunflower oil with 0.05% MMT | 0.091 | 0.489 | 0.978 | N/A | N/A | 0.0004 |
| | Cross Equation | Sunflower oil with 0.05% MMT | 1.517 | 0.608 | 0.358 | 0.1261 | 0.0741 | 0.0002 |
| Peanut | Power Law | Peanut oil with 0.05% MMT | 0.091 | 0.616 | 0.979 | N/A | N/A | 0.0002 |
| | Cross Equation | Peanut oil with 0.05% MMT | 0.095 | 0.804 | 1.947 | 0.0933 | 0.0829 | 0.0001 |
| Corn | Power Law | Corn oil with 0.05% MMT | 0.073 | 0.569 | 0.959 | N/A | N/A | 0.0006 |
| | Cross Equation | Corn oil with 0.05% MMT | 0.332 | 0.643 | 1.455 | 0.0795 | 0.0613 | 0.0006 |

From this table, it can be observed that the value of coefficient determination $R^2$ is close to 1 in cross equation model for all three cases. It can be concluded that, the more precise data can be obtained by using cross equation rather than power law model and this model seemed to be more accurate.

## 4.6 Tribological result

To observe the tribological result, sunflower, peanut, and corn oils were analyzed with and without the addition of Montmorillonite nanoclay at different concentrations (0.5%-3.0%). The experimental data were collected from block-on-ring tribotester under similar test conditions for each sample. The tribological tests were done using a load of 266N. For each sample, data of frictional force acting on block specimens, lubrication temperature and wear depth were gathered. There were different sensors to frictional force, lubrication temperature and wear depth.

To calculate wear volume Equation (5) is used which is shown in below,

$$Wear\ volume\ losss(mm^3) = \frac{mass\ of\ block\ before\ test(g) - mass\ of\ block\ after\ test(g)}{block\ density\ (g/mm^3)} \quad (5)$$

Here,

The density of the block specimen was taken as 8 g/cm$^3$. The initial and final block weights were recorded by measuring the mass of the blocks (Total of three times to get the more accurate result) before and after each test.

To find out the coefficient of friction (COF) average force acting on block was collected and calculated by using following Equation (6),

$$\mu = \frac{F_f}{F_N} \quad (6)$$

Here,

μ= The coefficient of friction.

$F_f$ = The frictional force acting on the block specimen.

$F_N$= The normal force acting on the block, 266 N.

### 4.6.1 Friction Force

Figures 30, 31 and 32 show the frictional force acting on the block specimen with and without the addition of MMT nanoparticle additives at different concentrations. The frictional force was gathered by the force sensor. In Figure 30, friction force vs time of base sunflower oil and the sunflower oil modified with MMT nanoparticles can be observed. Figures 31 and 32 show the similar plot for peanut and corn oils. In all three cases, it can be observed that the friction force acting on the block specimens was reduced by adding nanoparticles. One significant thing we have found was the difference of friction force among the base sunflower, peanut, and corn oil. The sunflower oil provided a higher friction force compared to that of peanut and corn oil. For all three oils, the frictional forces were seemed to be higher and over the time they decreased significantly both for the base and MMT modified nanoparticle. The MMT nanoparticles acted as a roller and formed a tribofilm which reduced the contact area and significantly reduced the frictional force.

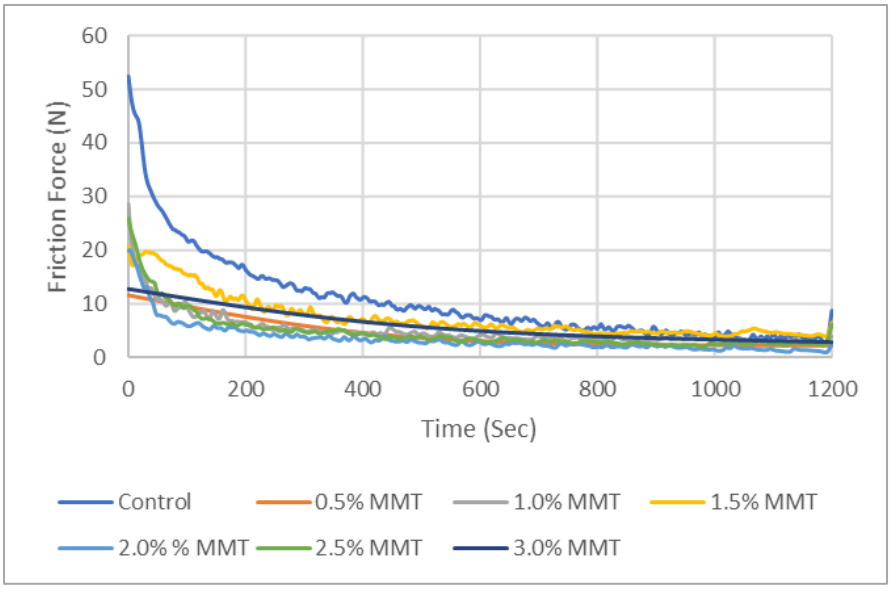


**Figure 30:** Friction force vs time for base sunflower oil and the sunflower oil modified with MMT nanoparticles.

The effects of the MMT nanoparticles at different concentrations on the frictional force vs time of the sunflower oil being used is shown in Figure 30. It can be easily observed that the MMT nanoparticles effectively reduced the frictional force in sunflower oil. The lowest frictional force was found to be at 2.00 wt.% MMT concentration. Another interesting point was that the 1.5 wt.% concentration had a higher frictional force at the end than that of the base sunflower oil. Moreover, the frictional force of nanolubricants never increased past the base sunflower oil friction force (except 1.5 wt.% at the end), having the lowest frictional force produced by the 2.00 wt.% MMT concentration as well.

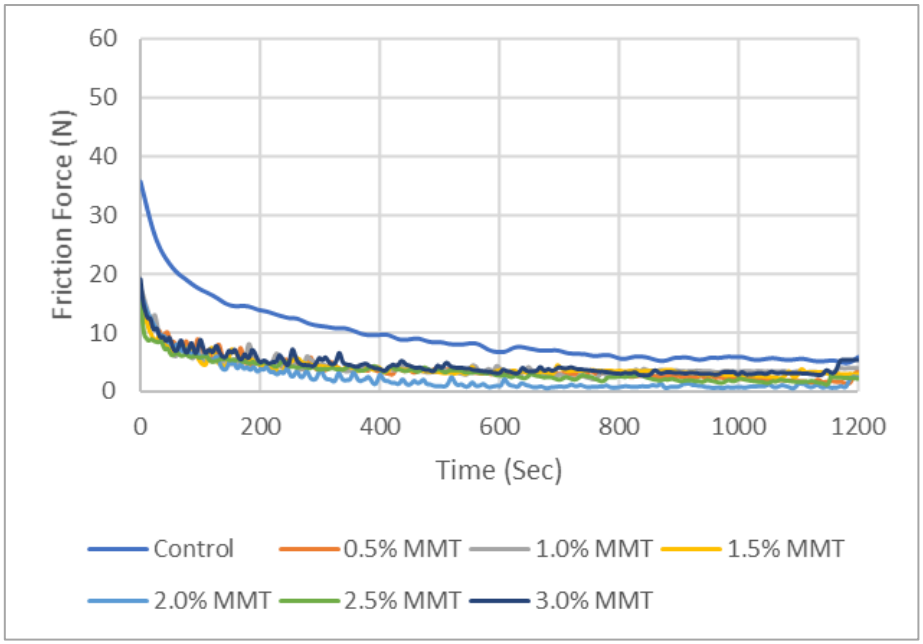


**Figure 31:** Friction Force vs time of base peanut oil and the peanut oil modified with MMT

The effects of the MMT nanoparticle additives at different concentrations on the frictional force vs time of the peanut oil being used is shown in Figure 31. In this case, it can be observed that the frictional force of the nanolubricants never increased past the base peanut oil throughout the experiment. Fatty acid composition of peanut oil could be the reason behind it. The lowest frictional force was observed at the 2.00 wt.% MMT concentration as well.

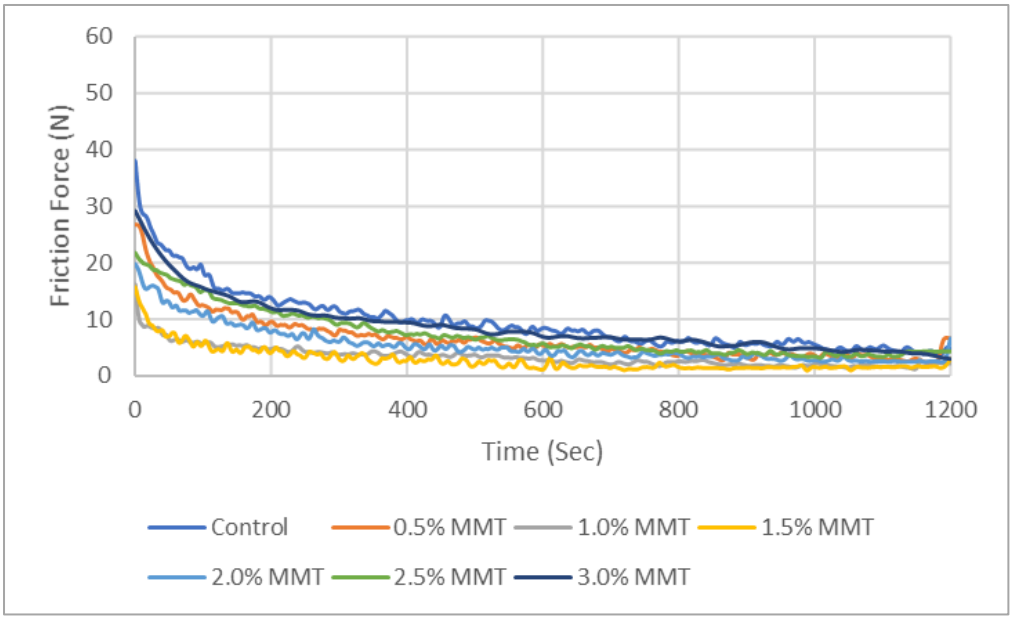


**Figure 32:** Friction Force vs time of base corn oil and the corn oil modified with MMT nanoparticles.

Friction force vs time of base corn oil and the corn oil modified with MMT nanoparticles can be seen in Figure 32. Corn oil exhibited the same characteristics as peanut oil and throughout the experiment, the temperature of nanolubricants were below than the base corn oil. The lowest frictional force was obtained at the 1.5 wt.% MMT concentration.

### 4.6.2 Coefficient of Friction (COF)

After getting the frictional force data from the force sensor, the coefficient of friction can be calculated using Equation 5. The coefficient of friction acting on the block specimens of MMT nanoparticles at various concentrations are shown in Figure 33a, b, and c. It can be observed that, the COF of base sunflower oil was higher than that of base peanut and corn oils, just like the frictional force. In all three cases, the COF results did not exhibit any kind of consistency. The optimum concentration for which the lowest COF was found was not the same.

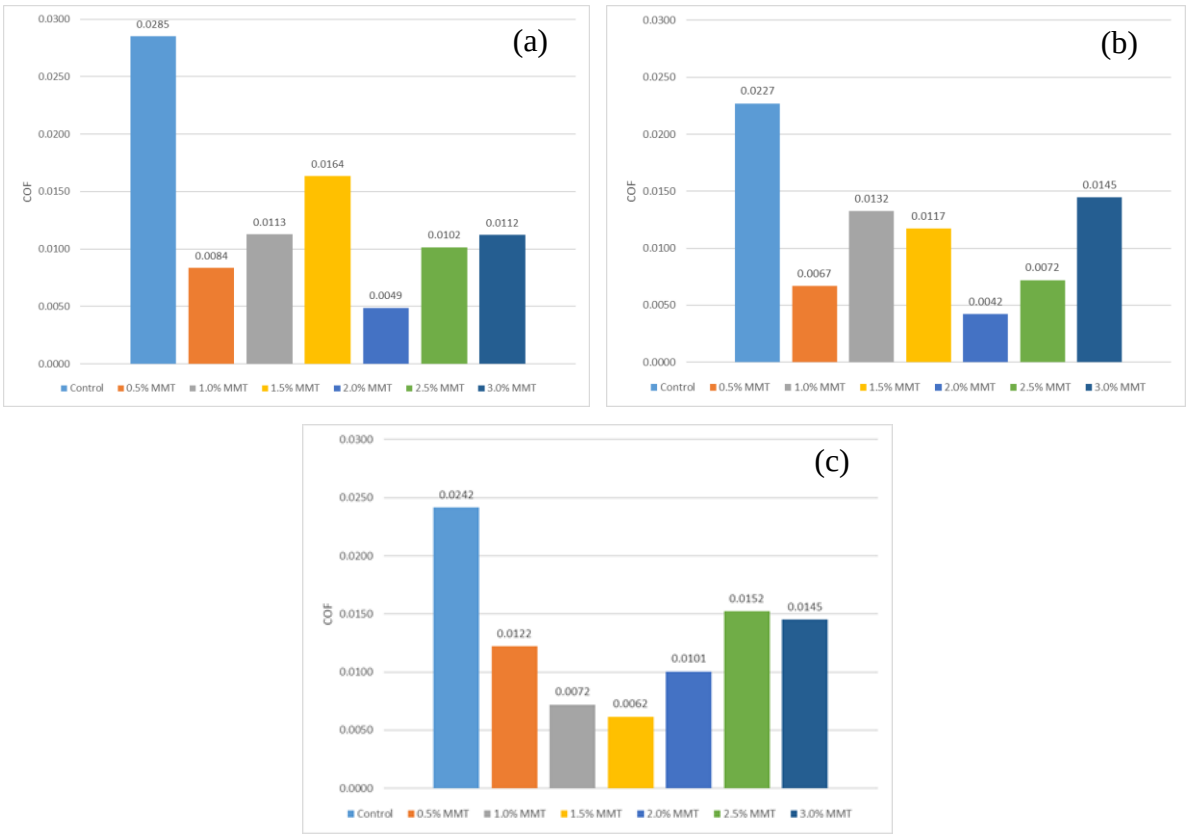


**Figure 33:** Coefficient of friction (COF) of base (a) sunflower oil, (b) peanut oil, and (c) corn oil and the corresponding oil modified with MMT nanoparticles.

For sunflower oil, the COF data showed an oscillating pattern in the concentrations of the MMT nanoparticle additive. The effects of the MMT nanoparticle at different concentrations on sunflower oil are shown in Figure 33a, and this figure exhibited an upside-down parabola effect. Sunflower oil without additives had a COF of 0.0285 which is higher than the other two base oils. At first, the COF decreased suddenly at 0.50 wt.% MMT concentration, then increased gradually up to 1.5 wt.% and the COF at 1.5 wt.% was 0.0164. After that, suddenly the COF decreased again at 2.0 wt.% and further increased after 2.0 wt.%. The addition of the MMT nanoparticles reduced the COF of the base sunflower oil from 0.0285 to 0.0049 and the lowest

COF was obtained at 2.0 wt.% concentration. The highest COF data for the nano-lubricant was found at 1.5 wt.% and the value was 0.0164. For sunflower oil, the optimal concentration was found to be at 2.0 wt.% and it reduced the COF of the base sunflower by 82.81%.

The effects of the MMT nanoparticle at different concentrations on peanut oil are shown in Figure 33b and it also exhibited the same kind of parabola effect as sunflower oil. Base peanut oil had the lowest COF compared to that of other two. Peanut oil without additives had a COF of 0.0227. Figure 33b is showing almost the same pattern as those found in the sunflower results. At the beginning, the COF decreased at 0.50 wt.%, then increased up to 1.5 wt.% and decreased again at 2.0 wt.%. After 2.0 wt.%, the COF started to increase again. The MMT nanoparticle reduced the COF of the base peanut oil from 0.0227 to 0.0042 which corresponds to the concentration of 2.0 wt.% of MMT. The highest COF for the nano-lubricant was found at 3.0 wt.% concentration and the value was 0.0145. The lowest COF was found to be at the 2.0 wt.% concentration, being able to decrease the peanut COF from 0.0227 to 0.0042. For peanut oil, the optimal concentration was 2.0 wt.%; it reduced the COF of the base peanut oil by 81.50%.

The effects of the MMT nanoparticle at different concentrations on corn oil are shown in Figure 33c. Corn oil without additives had a COF of 0.0242. Figure 33c shows a slightly different pattern as those found in the sunflower and peanut results. At the beginning, the COF decreased gradually up to 1.5 wt.% and then increased. The addition of the MMT nanoparticle lowered the COF of the base corn oil from 0.0242 to 0.0062 which corresponds to the concentration of 1.5 wt.% of MMT. Unlike sunflower and peanut, the addition of the MMT nanoparticle, as shown in Figure 33c, had opposite effect in which the particle concentrations followed a downside-up parabola effect. The highest COF for the nanolubricants was found to be at 2.5 wt.% concentration and the value was 0.0152. The lowest COF was found to be at the 1.5

wt.% concentration, being able to decrease the corn COF from 0.0242 to 0.0062. For corn oil, the optimal concentration was found to be 1.5 wt.%; it reduced the COF of the base corn oil by 74.38%.

### 4.6.3 Volumetric Wear

After measuring the weight of the blocks before and after each test, the volumetric wear can be measured using Equation 4.

From Figure 34, the mean volumetric wear of AISI 304 blocks lubricated with base oils and the corresponding oils modified with MMT nanoparticles can be observed. From the figure, one interesting behavior among the three base lubricants being used was noted, the base oils seemed to have the similar volume loss in all three cases. Moreover, the corn oil had better performance through the use of the MMT nanoparticles compared to the other two. Corn oil modified with MMT nanoparticles exhibited the highest volumetric wear loss that can be seen from Figure 34c and it reduced the wear by 82.16% at optimum concentration.

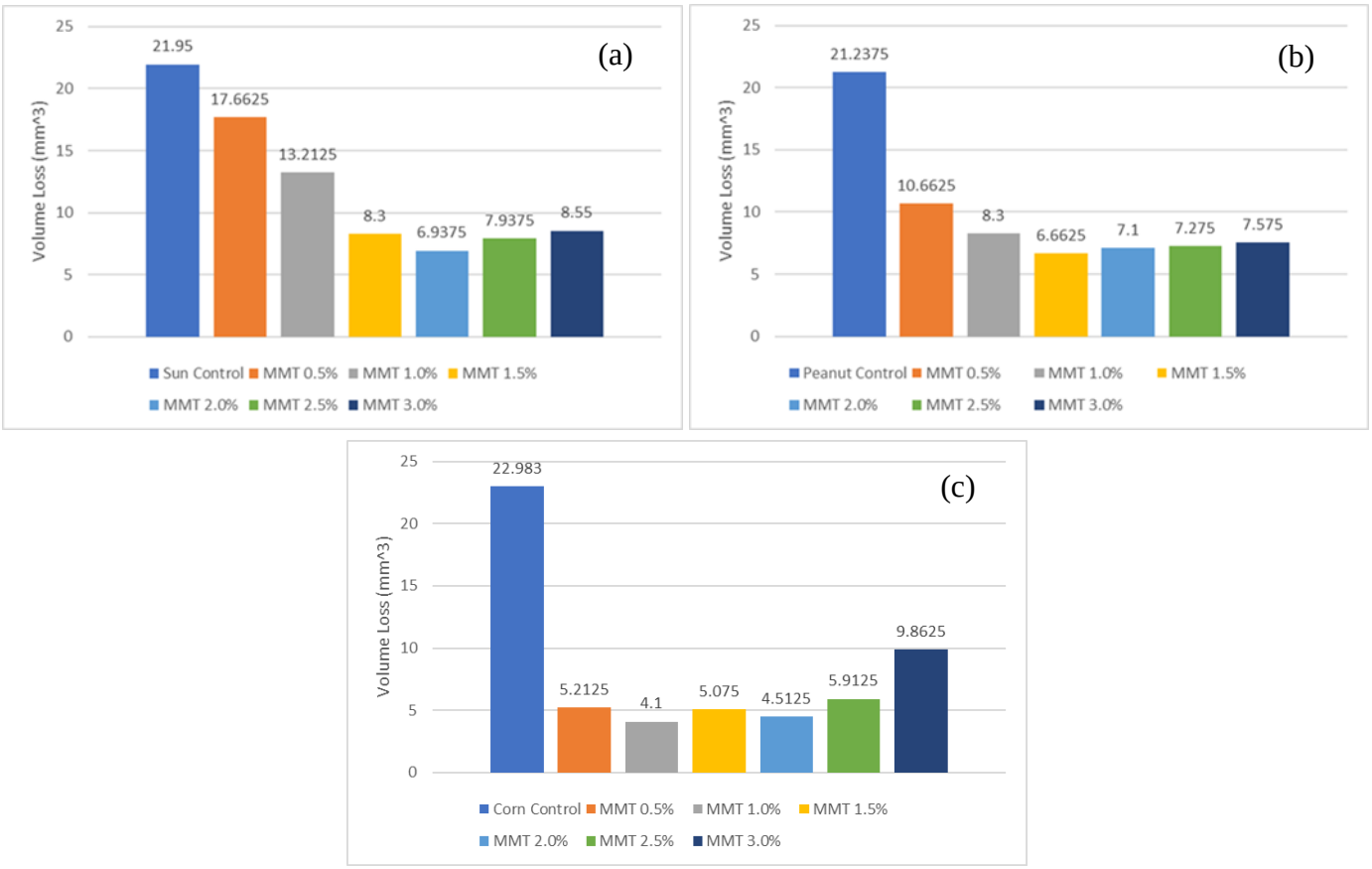


**Figure 34:** Volumetric wear loss of AISI 304 blocks lubricated with base (a) sunflower oil, (b) peanut oil, and (c) corn oil and the corresponding oil modified with MMT nanoparticles.

The mean volumetric wear loss of sunflower oil and sunflower oil modified with MMT nanoparticles is shown in Figure 34a. From the figure, it can be seen that the volumetric wear decreased up to 2.0 wt.% concentration and then started to increase again. The lowest volumetric wear can be observed at a concentration of 2.0 wt.%, reducing the amount of wear by 68.39%. The addition of the MMT nanoparticle exhibited a downside up parabola effect, according to the findings.

For peanut oil, the addition of the MMT nanoparticle exhibited the similar kind of parabola effect like sunflower oil. The mean volumetric wear loss of peanut oil and peanut oil modified with MMT nanoparticles is shown in Figure 34b. The volumetric wear decreased up to

1.5 wt.% concentration and then started to increase again. The optimal concentration can be viewed at 1.5 wt.% for peanut oil. The addition of the MMT nanoparticles was able to lower the volumetric loss by 68.63% at optimum concentration.

For corn oil, the effects of the MMT nanoparticle at different concentrations on mean volumetric wear loss can be observed in Figure 34c. The volumetric wear decreased up to 1.0 wt.% concentration and then started to increase again. The optimal concentration can be viewed at 1.0 wt.% for peanut oil and the addition of the MMT nanoparticles was able to lower the volumetric loss by 82.16% which is higher compared to that of sunflower and peanut oil.

### 4.6.4 Lubricant Temperature

Lubrication temperature vs time of base oils and the corresponding oils modified with MMT nanoparticles can be observed in Figures 35, 36 and 37. During the tribological test, a temperature sensor was used to measure the temperature of the lubricant during experiments to analyze the lubrication behavior of nano-lubricants. For all vegetable oil-based nano-lubricants, the addition of Montmorillonite nanoclay seemed to lower the base temperature of the lubricant, according to the experimental results obtained. As MMT nanoparticle reduced the friction by reducing the contact area of the mechanical parts, it could be the reason of exhibiting lower temperature in nanolubricants. Among the three base oils, corn oil exhibited the highest lubrication temperature and sunflower oil exhibited the lowest.

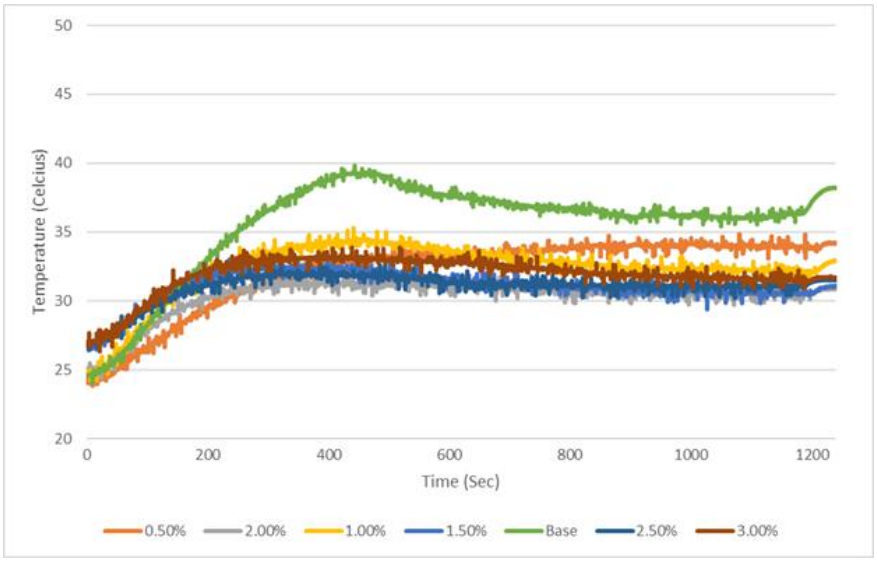


**Figure 35:** Lubrication temperature vs time of base sunflower oil and the sunflower oil modified with MMT nanoparticles.

Figure 35 shows the lubrication temperature profile for base sunflower oil and sunflower oil modified with MMT nanoparticle. From the figure, it can be seen that the base oil lubrication temperature was higher compared to the other nanolubricants modified with MMT nanoparticle. The base lubrication temperature seemed significantly higher than others and it fluctuated a lot. With addition of MMT nanoparticles, the lubrication temperature reduced significantly than its base lubrication temperature. Though all the initial lubrication temperature were nearly similar, the final temperature was quite different for each lubricant. For nano lubricants which contains of 2.0 wt.% MMT shows the maximum decrease in lubrication temperature which is approximately 18.5% less compared to the final temperature of base sunflower lubrication temperature. The lubrication temperature profile also shows that the lubrication temperature rises with time and then turns into a steady state condition in every case.

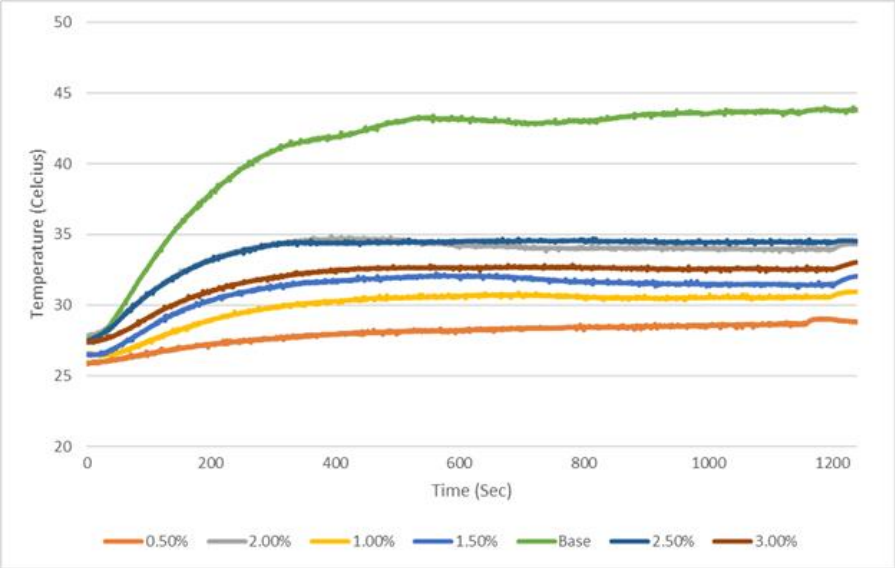


**Figure 36:** Lubrication temperature vs time of base peanut oil and the peanut oil modified with MMT nanoparticles.

In case of peanut oil shown in Figure 36, the base oil lubrication temperature was significantly higher compared to other nanolubricants modified with MMT nanoparticles and it did not fluctuate much. The temperature profile in all cases showed a steady behavior for peanut oil but it didn't follow any linear pattern. With addition of MMT, the lubrication temperature is decreased and for 0.5 wt.% of MMT shows the maximum decrease in lubrication temperature which is approximately 38.6% less compared to the final temperature of base peanut oil temperature.

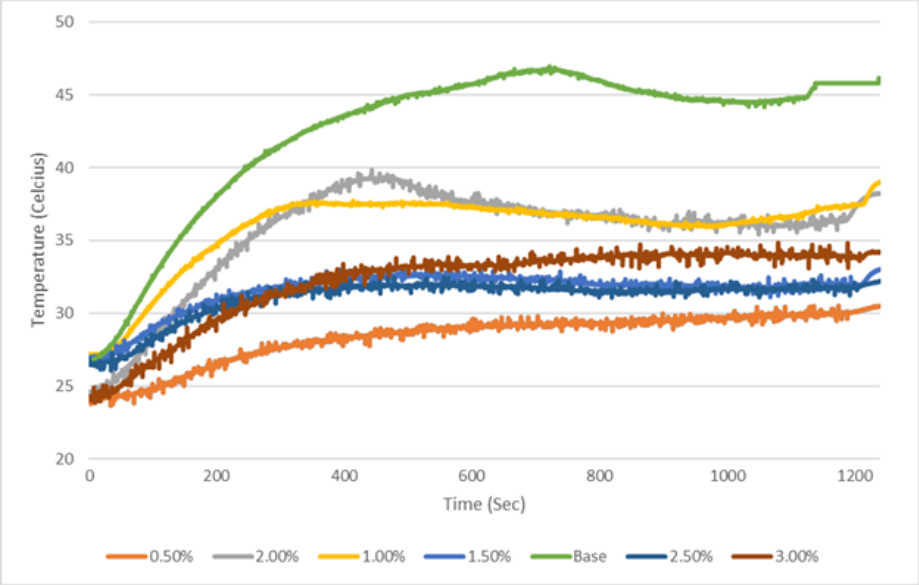


**Figure 37:** Lubrication temperature vs time of base corn oil and the corn oil modified with MMT nanoparticles.

In Figure 37, from lubrication temperature profile of corn oil, it can be observed that lubrication temperature of corn base oil is higher compared to other corn lubricants modified with MMT nanoparticle. For MMT concentration of 0.5 wt.% exhibits lowest lubrication temperature and it reduced the temperature approximately 32.6% less compared to the final temperature of base corn oil temperature. For all concentration of MMT, lubrication temperature is decreased but it does not follow any linear pattern as well.

## 4.7 Wear Surface Characterization:

Wear surface characterization of the wear scars of the blocks was performed by SEM analysis and roughness test. For each of the lubricants, eight blocks were tested (total of 24 blocks), and analyzing the wear scars of all blocks would require a lot of time. For this reason, to complete the wear surface characterization, only the best concentrations due to the volumetric wear and controls for each vegetable oil group were analyzed. From the tribological results, it

was found that for sunflower oil, the best concentration of MMT nanoparticle was found to be at 2.0 wt.%. For peanut and corn oil, the best concentrations of MMT nanoparticles were found to be at 1.5wt.% and 1.0 wt.%. After selecting the blocks corresponding to the base oil and their best concentration, SEM analysis and roughness test of the wear scars could be done.

### 4.7.1 SEM of The Wear Scars:

The worn surfaces of the blocks were further investigated by the SEM analysis under different magnification. The SEM images of the wear scar of base sunflower, peanut, and corn oil under different magnification are shown in Figure 38. In case of sunflower, peanut, and corn base it can observed that there were large number of burrs and furrows which resulted in increase in friction and wear. In the absence of a tribofilm, the wear track for the base lubricant exhibited numerous grooves and furrows caused by adhesive wear on the surface of the lubricants. This burrs and furrows increased the friction between sliding surfaces.

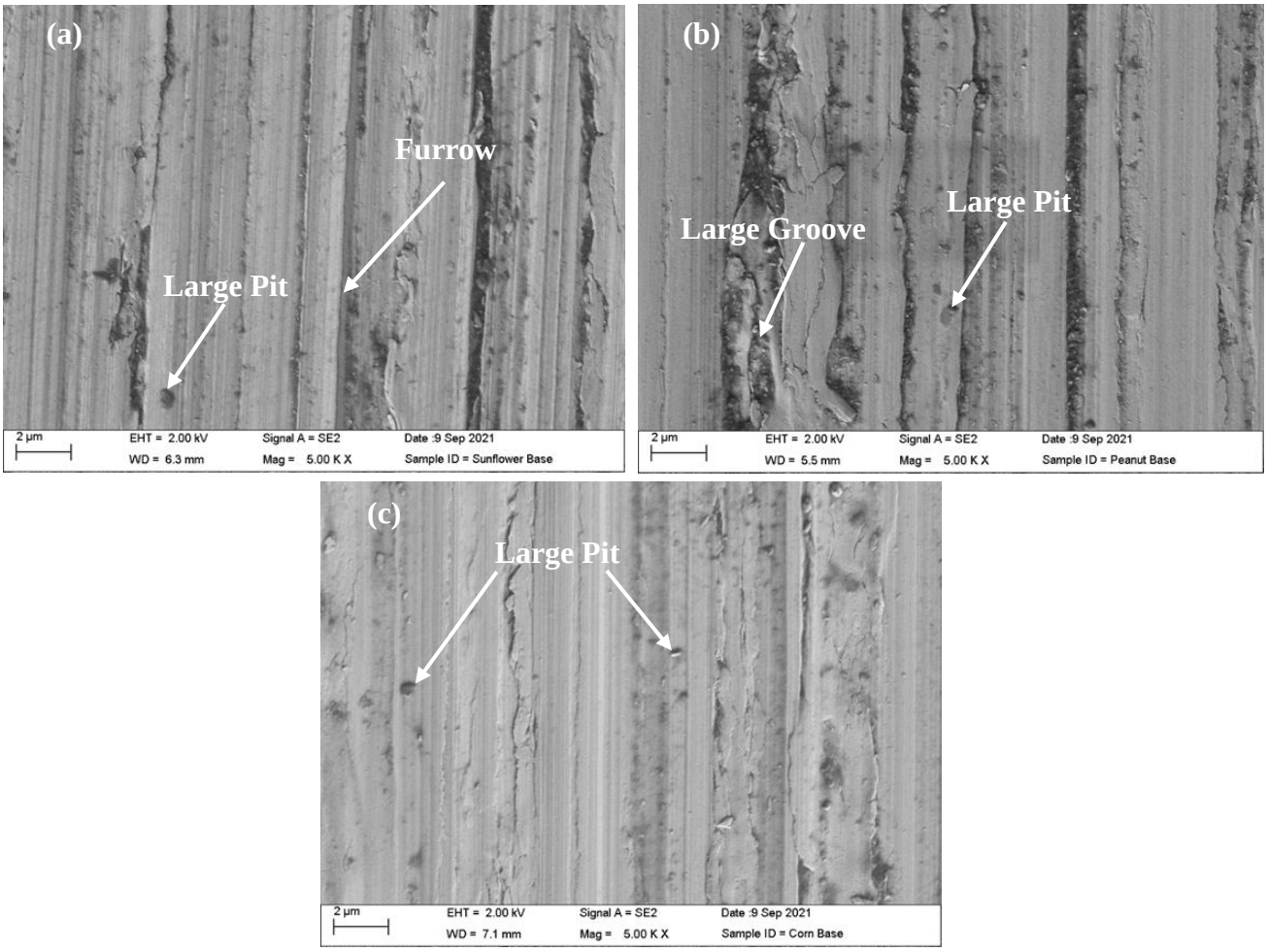


**Figure 38:** SEM micrographs of worn surfaces on block lubricated with: (a) sunflower oil, (b) peanut oil, and (c) corn oil.

Figure 39 shows SEM images of wear scar of the blocks lubricated with best concentration nano lubricant of sunflower, peanut, and corn oil due to the volumetric wear. After incorporating MMT nanoparticles, furrow-depth and metal burr have both decreased significantly, as can be seen in Figure 33. In case of 2.0 wt.% MMT modified sunflower oil, 1.5 wt.% MMT modified peanut oil and 1.0 wt.% MMT modified corn oil, the wear scar has limited number of burrs and furrows which helped to reduce the frictional force as well as low volumetric wear. On the surface of used blocks, it also observed that a smaller number of grooves also present compared to base oil used blocks. The exfoliation occurs on the surface of

the block of best modified nano lubricant also helps to reduce the overall friction during the lubrication.

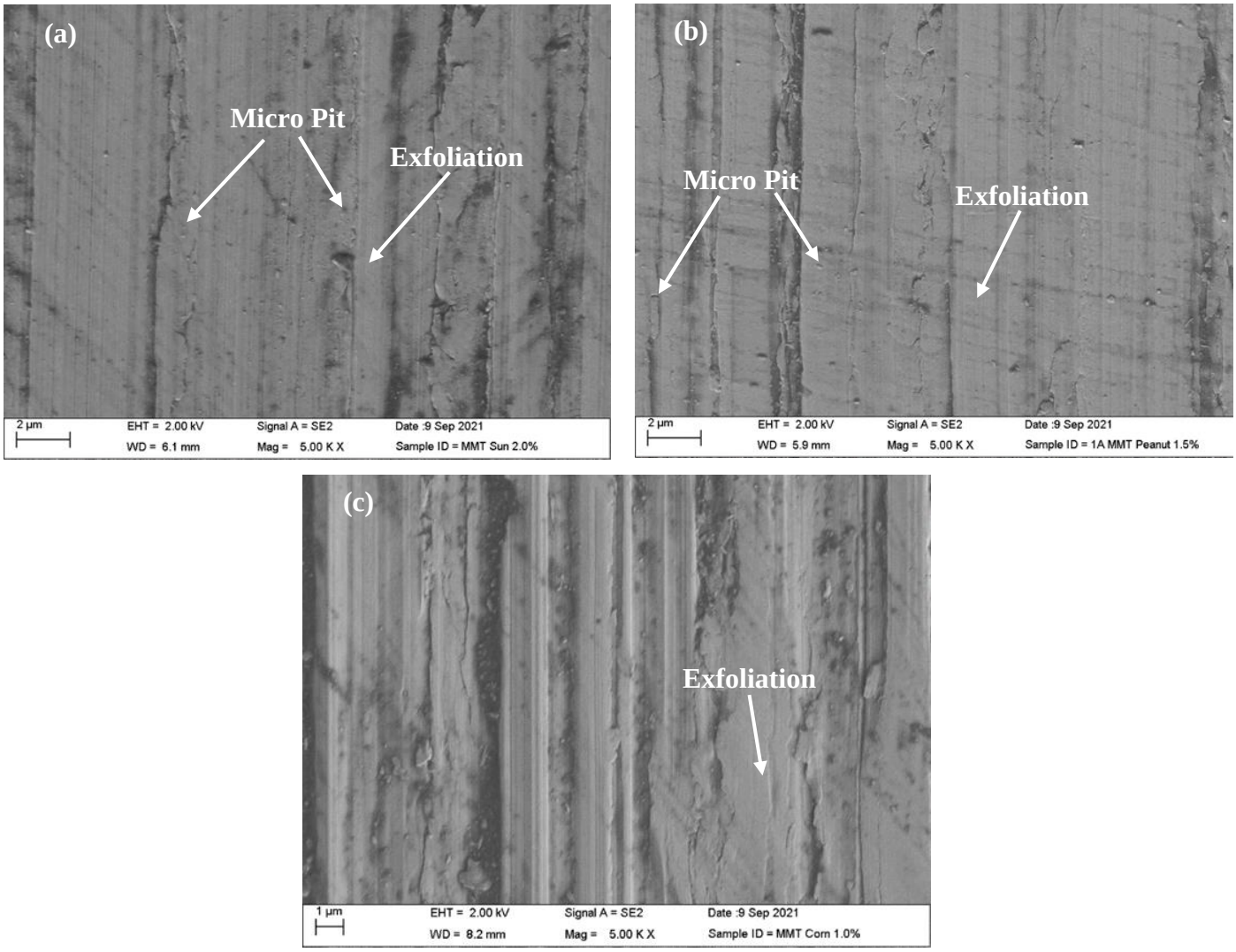


**Figure 39:** SEM micrographs of worn surfaces on block lubricated with: (a) sunflower oil, (b) peanut oil, and (c) corn oil nano-lubricants.

### 4.7.2 Roughness (Before and After Wear Test):

A MarSurf M300C profilometer as shown in Figure 17 was used to quantify the average surface roughness of AISI 304 Blocks lubricated with base oils and the corresponding oils modified with the best concentration due to the volumetric wear. The nanoparticles present numerous asperities seemed to reduce the amount of roughness when compared to the initial roughness of the blocks.

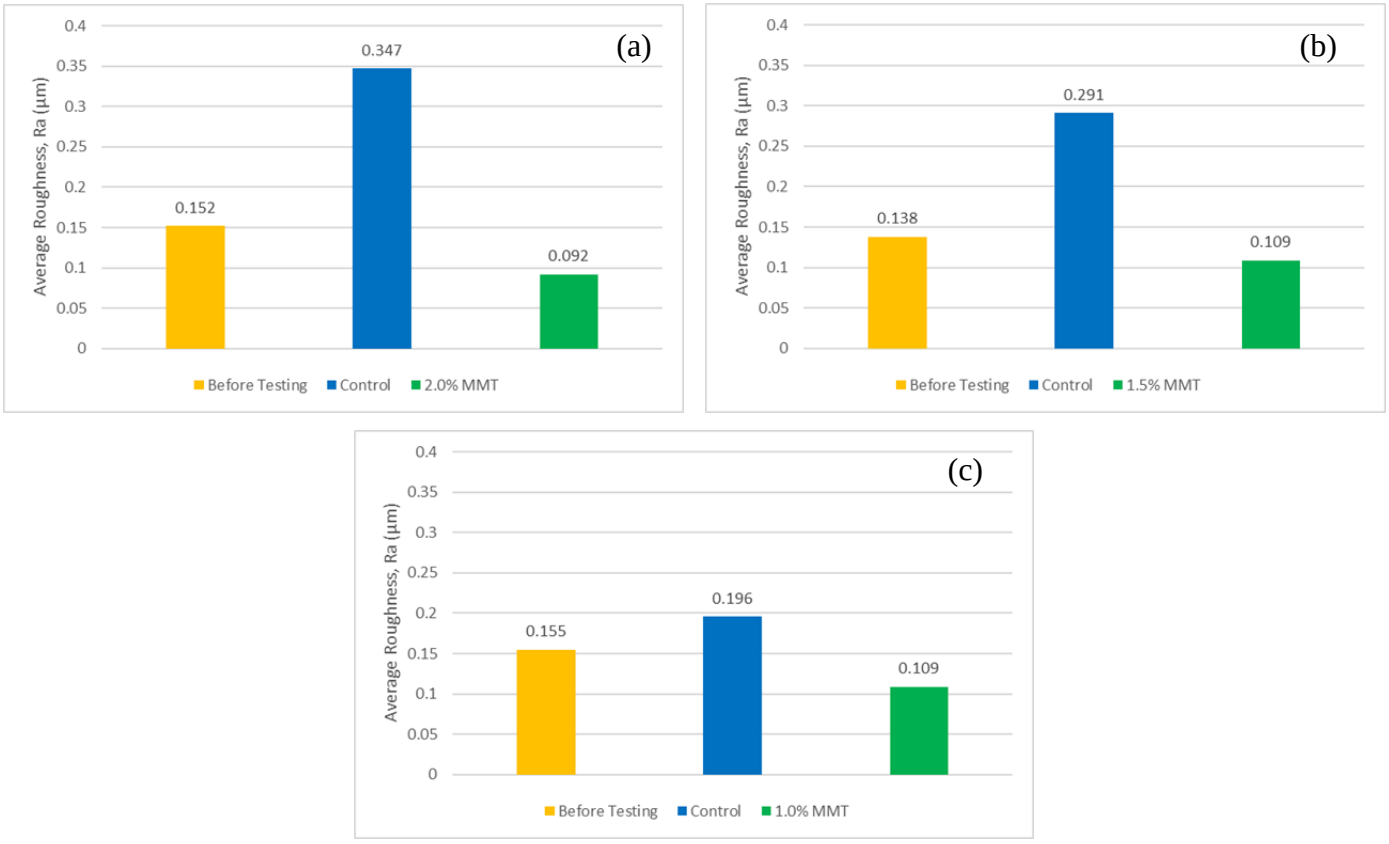


**Figure 40:** Average surface roughness of AISI 304 Blocks lubricated with (a) sunflower oil, (b) peanut oil, and (c) corn oil and the corresponding oil modified with the best concentration due to the volumetric wear.

When compared to the controlled untested sample, it can be seen in Figure 40a that base sunflower oil significantly increased the roughness of the block by 128.29%. The best

concentration was found to be at 2.0 wt.% due to the volumetric wear. For 2.0 wt.% MMT modified sunflower oil, the roughness was decreased by 39.47%. From Figure 40b, in case of peanut oil, the addition of the MMT nanoparticles decreased the roughness of the block. At first, the base peanut oil increased the roughness of the block by 110.87% when compared to controlled untested sample. The best concentration was found to be at 1.5 wt.% due to the volumetric wear. For 1.5 wt.% MMT modified peanut oil, the roughness was decreased by 21.01%. the similar observation was found in case of corn oil as shown in Figure 40c. At first, the base corn oil increased the roughness of the block by 26.45% when compared to controlled untested sample. For 1.0 wt.% MMT modified corn oil, the roughness was decreased by 29.67%.

The incorporation of MMT nanoparticles into the lubricants reduced the roughness of the lubricating surface significantly by nanoparticle-assisted abrasion i.e., polishing effect. In this mechanism, the nanoparticles polish the rubbing surface. The polishing effect helps to remove any asperities that can be found on the surface of the blocks to reduce the friction and to smoothen out surface of the material [28].

## 4.8 Tapping Torque Test

The tapping torque tests conducted in Grizzly milling machine as shown in Figure 16 and followed ASTM standard. To perform the tapping torque test with all the respective concentrations of the nanolubricants took a lot of time. For this reason, the performance of sunflower oil, peanut oil, and corn oil in terms of tapping torque was evaluated with base oil and the best performing nano lubricants with their respective concentrations due to the volumetric wear. When doing the tapping torque test, the force sensor of the custom-made tapping torque tester provided the force acting on the aluminum specimen. To obtain the torque, the force needed to be multiplied with a distance which can easily be done from Equation 7,

$$T = F * D \quad (7)$$

Here,

$T$= The torque.

$F$= The force obtained from the force sensor.

$D$= The distance of the moment arm attached to the specimen holder.

The tapping torque results conducted in Grizzly Milling machine can be observed on Figure 4. The time required by each test to complete the tapping to the aluminum specimen for different base oil was almost same. From the figure, it can also be observed that base corn oil showed much higher torque compared to that of sunflower and peanut oil. During roughness test, it can be seen that corn oil produced much less roughness and it could be the reason of showing higher torque.

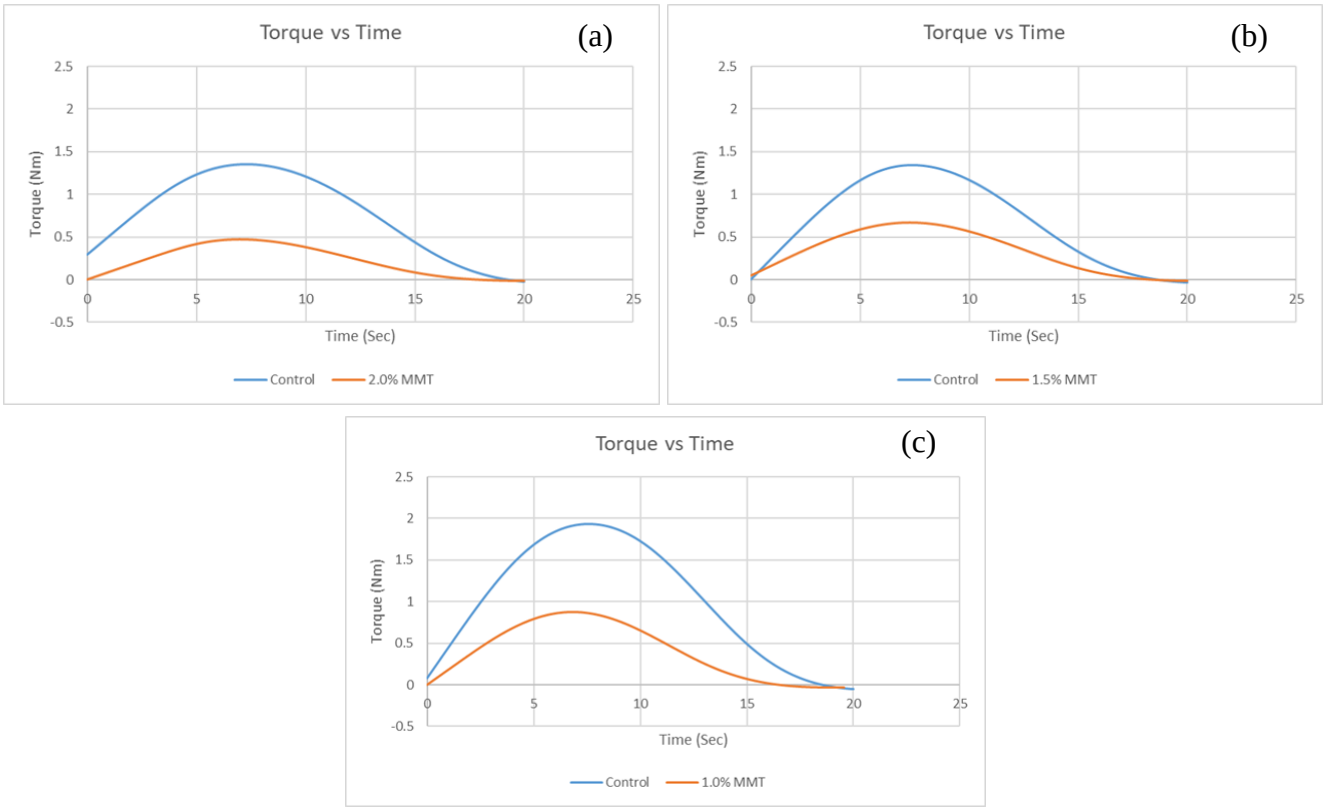


**Figure 41:** Tapping torque vs time of base (a) sunflower oil, (b) peanut oil, and (c) corn oil and the corresponding oil modified with the best concentration due to the volumetric wear.

From the Figure 42, it can be observed that among all base oils, corn oil shows maximum tapping torque of 1.93 Nm acting on the specimen. The base sunflower oil and base peanut oil shows almost the same tapping torque and the approximate value is 1.357 Nm and 1.347 Nm. From Figure 40, it can be seen that the corn oil produced less roughness compared to the other two and in turn caused the Grizzly mill to use less energy to perform the tests. For this reason, corn oil showed higher torque. The best concentration due to the volumetric wear was found to be at 2.0 wt.%, 1.5 wt.%, 1.0 wt.% for sunflower, peanut, and corn oil respectively. Figure 42 shows that the tapping torque for 2.0 wt.% MMT sunflower nano lubricant is lower than the base

oil. The maximum tapping torque for sunflower oil best concentration was found 0.471 Nm which is 65.3% lower than the maximum torque produced by sunflower base oil. In Figure 36, for peanut best concentration nano lubricant, tapping torque is 0.673 Nm which is 50.03% lower than the maximum torque produced by peanut base oil. In case of corn oil, the best concentration MMT nano lubricant in Figure 42 shows the maximum tapping torque of 0.874 Nm which is 54.72% lower than the base corn oil torque.

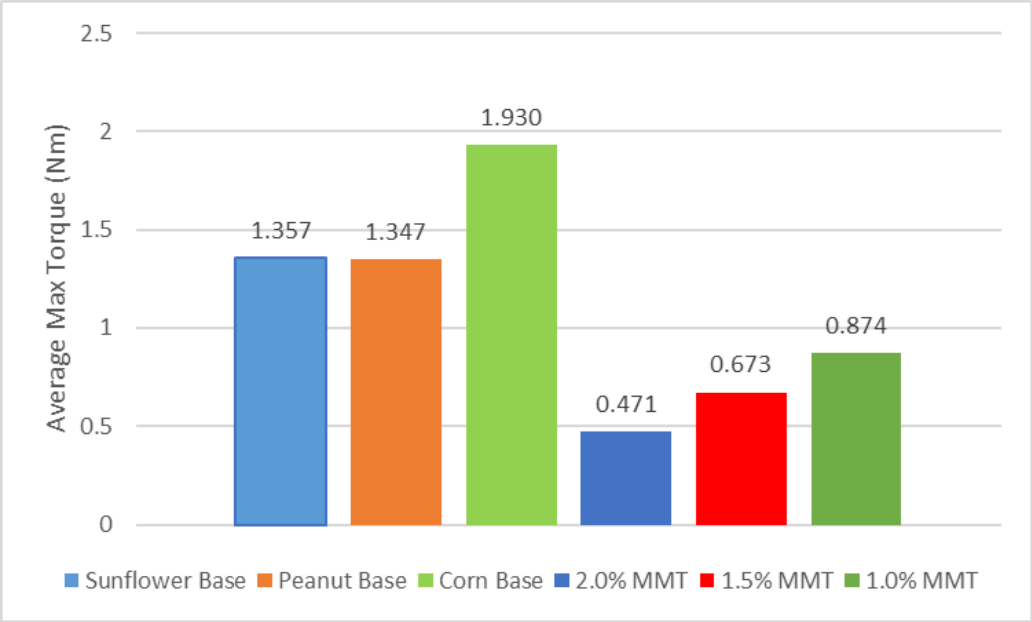


**Figure 42:** Average maximum torque of sunflower oil, peanut oil, corn oil and the corresponding oil modified with the best concentration due to the volumetric wear.

The similar types of results can be found when $MoS_2$ nanotubes were used during form tapping of zinc coated automotive components [29]. The incorporation of nanotubes significantly reduced the tapping toque of the system in this study which was quite similar what we have found in our study. In another study, modified jatropha oil exhibited a reduction of

average tapping torque of the system when compared to synthetic ester and crude jatropha oil [30].

# CHAPTER V

# CONCLUSIONS

The current study demonstrated that the addition of MMT nanoparticles can be effective to the tribological and rheological process and can provide optimal result. As a replacement for petroleum, mineral and synthetic oil, vegetable oils enhanced with MMT nanoparticles show a great potentiality to develop new low cost and environmentally friendly nanomaterial-based nanolubricants. The following research can be summarized as follows:

- The concentration of MMT nanoparticles affects the viscosity of nanolubricants. The viscosity of sunflower and corn oil increased with the addition of MMT nanoparticles and appeared to maintain a shear thinning characteristic. The highest viscosity was found to be at 0.10 wt.% concentration. The peanut oil exhibited an opposite characteristic. The addition of MMT nanoparticles to peanut oil reduced the viscosity of the nano-lubricants while maintaining a shear thinning effect similar to the other two and the lowest viscosity was found to be at 0.01 wt.% concentration.
- MMT nanoparticle concentration has a significant impact on the tribological properties of nanolubricants as well. Increasing the concentration of MMT in lubricants enhances the tribological property which generally increases until a specific concentration is reached and drops. They reduced the wear volume loss by 68.39%, 68.63%, 82.16% and coefficient of friction (COF) by 82.21%, 81.50%,74.38% respectively. Up to a certain concentration, increasing nanoparticle concentration in lubricants reduces both wear and COF, and then

both characteristics increase. But the optimum concentration may not be the same for the two properties.

- MMT nanoparticles seemed to reduce the surface roughness compared to the initial roughness of the blocks. The MMT modified nano-lubricant reduced the roughness of the blocks by 39.47%, 21.01%, 29.67% for sunflower, peanut, and corn oil respectively. Similar results can be observed by SEM analysis of worn-down specimens.
- MMT nanoparticles showed promising effect in reducing the tapping torque of the system. The addition of the nanoparticles to the vegetable oils (sunflower, peanut, and corn) decreased the torque acting in the system. They reduced the maximum torque of the system by 65.3%, 50.03% and 54.72% respectively. Corn oil produced the higher torque compared to the other two because less energy was required in this case to complete the test due to its less roughness.

## 5.1 Future Work:

In this research, single additive nanoparticle has been used which may be replaced by hybrid nanoparticle in future. Moreover, further analysis can be done to find the thermal properties of the nano-lubricants which can be used through heat transfer equations to gather more accurate information on the friction forces acting on the block specimens. As nanoparticles tend to agglomerate, maintaining the stability of nanoparticles in lubricant for an extended period of time is a difficult issue. Further research can be done on nanoparticles stability and the sedimentation problems found in the different nano-lubricants.

REFERENCES


[1] F. Archibald, “History of lubrication,” *Lubrication Engineering*, vol. 55, no. 9, pp. 9–10, 1999, Accessed: Nov. 09, 2021. [Online]. Available: https://www.proquest.com/docview/226945291?pq-origsite=gscholar&fromopenview=true

[2] S. M. Hsu, “Nano-lubrication: Concept and design,” *Tribology International*, vol. 37, no. 7, pp. 537–545, Jul. 2004, doi: 10.1016/J.TRIBOINT.2003.12.002.

[3] S. P. Darminesh, N. A. C. Sidik, G. Najafi, R. Mamat, T. L. Ken, and Y. Asako, “Recent development on biodegradable nanolubricant: A review,” *International Communications in Heat and Mass Transfer*, vol. 86, pp. 159–165, Aug. 2017, doi: 10.1016/J.ICHEATMASSTRANSFER.2017.05.022.

[4] “Lubricants History<Basic Information<Lube Intelligence | S-OIL SEVEN,” *oil sevem*. http://www.s-oil7.com/eng/knowledge/basic/history.jsp (accessed Nov. 09, 2021).

[5] B. Zareh-Desari and B. Davoodi, “Assessing the lubrication performance of vegetable oil-based nano-lubricants for environmentally conscious metal forming processes,” *Journal of Cleaner Production*, vol. 135, pp. 1198–1209, Nov. 2016, doi: 10.1016/J.JCLEPRO.2016.07.040.

[6] V. Cortes, K. Sanchez, R. Gonzalez, M. Alcoutlabi, and J. A. Ortega, “The performance of SiO2 and TiO2 nanoparticles as lubricant additives in sunflower oil,” *Lubricants*, vol. 8, no. 1, Jan. 2020, doi: 10.3390/LUBRICANTS8010010.

[7] T. Trzepieciński, “Tribological performance of environmentally friendly bio-degradable lubricants based on a combination of boric acid and bio-based oils,” *Materials*, vol. 13, no. 17, Sep. 2020, doi: 10.3390/MA13173892.

[8] R. J. Hamilton, “Structure and general properties of mineral and vegetable oils used as spray adjuvants,” *Pesticide Science*, vol. 37, no. 2, pp. 141–146, 1993, doi: 10.1002/PS.2780370206.

[9] M. H. Jabal, A. R. Abdulmunem, and H. S. Abd, “Experimental investigation of tribological characteristics and emissions with nonedible sunflower oil as a biolubricant,” *Journal of the Air and Waste Management Association*, vol. 69, no. 1, pp. 109–118, Jan. 2019, doi: 10.1080/10962247.2018.1523070.

[10] A. R. Service. U.S. Department of Agriculture, “FoodData Central,” *FoodData Central*, 2019. https://fdc.nal.usda.gov/ (accessed Nov. 09, 2021).

[11] “The best oils to use for cooking, according to nutritionists.” Accessed: Nov. 09, 2021. [Online]. Available: https://www.nbcnews.com/better/lifestyle/best-oils-use-your-cooking-according-nutritionists-ncna1032426

[12] “Smoke Points of Cooking Oils and Fats - Jessica Gavin.” https://www.jessicagavin.com/smoke-points-cooking-oils/ (accessed Nov. 09, 2021).

[13] Y. J. J. Jason, H. G. How, Y. H. Teoh, and H. G. Chuah, “A study on the tribological performance of nanolubricants,” *Processes*, vol. 8, no. 11, pp. 1–33, Nov. 2020, doi: 10.3390/PR8111372.
[14] W. Dai, B. Kheireddin, H. Gao, and H. Liang, “Roles of nanoparticles in oil lubrication,” *Tribology International*, vol. 102, pp. 88–98, Oct. 2016, doi: 10.1016/J.TRIBOINT.2016.05.020.
[15] V. Cortes and J. A. Ortega, “Evaluating the rheological and tribological behaviors of coconut oil modified with nanoparticles as lubricant additives,” *Lubricants*, vol. 7, no. 9, Sep. 2019, doi: 10.3390/LUBRICANTS7090076.
[16] K. Lee *et al.*, “Understanding the role of nanoparticles in nano-oil lubrication,” *Tribology Letters*, vol. 35, no. 2, pp. 127–131, Aug. 2009, doi: 10.1007/S11249-009-9441-7.
[17] G. Liu, X. Li, B. Qin, D. Xing, Y. Guo, and R. Fan, “Investigation of the mending effect and mechanism of copper nano-particles on a tribologically stressed surface,” *Tribology Letters*, vol. 17, no. 4, pp. 961–966, Nov. 2004, doi: 10.1007/S11249-004-8109-6.
[18] X. Tao, Z. Jiazheng, and X. Kang, “The ball-bearing effect of diamond nanoparticles as an oil additive,” *Journal of Physics D: Applied Physics*, vol. 29, no. 11, pp. 2932–2937, Nov. 1996, doi: 10.1088/0022-3727/29/11/029.
[19] M. Calabi Floody, B. K. G. Theng, P. Reyes, and M. L. Mora, “Natural nanoclays: applications and future trends – a Chilean perspective,” *Clay Minerals*, vol. 44, no. 2, pp. 161–176, Jun. 2009, doi: 10.1180/CLAYMIN.2009.044.2.161.
[20] M. S. Nazir, M. H. Mohamad Kassim, L. Mohapatra, M. A. Gilani, M. R. Raza, and K. Majeed, “Characteristic Properties of Nanoclays and Characterization of Nanoparticulates and Nanocomposites,” pp. 35–55, 2016, doi: 10.1007/978-981-10-1953-1_2.
[21] L. Pena-Paras, D. Maldonado-Cortes, F. Castillo, J. Leal, and S. Garza, “Application of nanoclay lubricants for lowering wear of tools for steel meshing - A case study,” *IOP Conference Series: Materials Science and Engineering*, vol. 400, no. 7, Sep. 2018, doi: 10.1088/1757-899X/400/7/072004.
[22] Z. Cao, Y. Xia, and X. Xi, “Nano-montmorillonite-doped lubricating grease exhibiting excellent insulating and tribological properties,” *Friction*, vol. 5, no. 2, pp. 219–230, Jun. 2017, doi: 10.1007/S40544-017-0152-Z.
[23] Y. University, “XRD | West Campus Materials Characterization Core,” *Yale University*, 2021. https://ywcmatsci.yale.edu/xrd (accessed Dec. 07, 2021).
[24] M. S. H. Akash and K. Rehman, “Thermo Gravimetric Analysis,” *Essentials of Pharmaceutical Analysis*, pp. 215–222, 2020, doi: 10.1007/978-981-15-1547-7_19.
[25] M. D. la Cruz, R. Gonzalez, J. A. Gomez, A. Mendoza, and J. A. Ortega, “Design and Validation of A Modular Instrument to Measure Torque and Energy Consumption in Industrial Operations,” *Instruments 2019, Vol. 3, Page 41*, vol. 3, no. 3, p. 41, Aug. 2019, doi: 10.3390/INSTRUMENTS3030041.
[26] P. A. Azar, F. Farjami, M. Saber Tehrani, and E. Eslami, “A carbon nanocomposite ionic liquid electrode based on montmorillonite nanoclay for sensitive voltammetric determination of thioridazine,” *International Journal of Electrochemical Science*, vol. 9, no. 5, pp. 2535–2547, 2014, Accessed: Nov. 09, 2021. [Online]. Available: https://www.researchgate.net/publication/286048899_A_Carbon_Nanocomposite_Ionic_Liquid_Electrode_Based_on_Montmorillonite_Nanoclay_for_Sensitive_Voltammetric_Determination_of_Thioridazine

[27] B. A. Fil, C. Özmetin, and M. Korkmaz, “Characterization and electrokinetic properties of montmorillonite,” *Bulgarian Chemical Communications*, vol. 46, no. 2, pp. 258–263, 2014.
[28] A. Tcherbi-Narteh, M. Hosur, and S. Jeelani, “Effects of Different Montmorillonite Nanoclay Loading on Cure Behavior and Properties of Diglycidyl Ether of Bisphenol A Epoxy,” *Journal of Nanomaterials*, vol. 2016, 2016, doi: 10.1155/2016/3840348.
[29] “Sci-Hub | Performance of nanolubricants containing MoS2 nanotubes during form tapping of zinc-coated automotive components. Journal of Manufacturing Processes, 39, 167–180 | 10.1016/j.jmapro.2019.02.012.” https://sci-hub.se/http://dx.doi.org/10.1016/j.jmapro.2019.02.012 (accessed Dec. 08, 2021).
[30] N. Talib, R. M. Nasir, and E. A. Rahim, “Tribological behaviour of modified jatropha oil by mixing hexagonal boron nitride nanoparticles as a bio-based lubricant for machining processes,” *Journal of Cleaner Production*, vol. 147, pp. 360–378, Mar. 2017, doi: 10.1016/J.JCLEPRO.2017.01.086.

# APPENDIX

# APPENDIX

## STATE OF THE ART EQUIPMENT AND SOFTWARE

State-of-the-Art Equipment

| Equipment | Purpose | Results Obtained |
|---|---|---|
| HAAKE RS-150 RheoStress | Measure the viscosity at different shear rates of base sunflower, peanut, and corn oil modified with MMT nanoparticles. | Viscosity of lubricants at shear rates of 10 to 120 s-1 of base sunflower, peanut, and corn oil modified with MMT nanoparticles. |
| XS205DU Electronic Balance | Balance to measure samples, and nanolubricants. | Sample weights as well as particle concentration weights were obtained to find the volumetric wear. |
| 120 Sonic Dismembrator | To mix lubricant solutions. | Mixed MMT nanoparticles into the vegetable oil used, obtaining a mixed solution. |
| Nano 1200T grinder polisher | Remove any impurities and gain similar surface textures for each of the block specimens. | Smooth surfaces of the blocks for tribological test. |
| Ultrasonic Cleaner | Remove any dirt, grease, or other factors that can affect the weight of the blocks. | Blocks without any kind of dirt, polishing compounds. |
| Custom-made Tribotester | Measure the tribological behavior of base sunflower, peanut, and corn oil modified with MMT nanoparticles. | Frictional force, lubricant temperature, and wear of base sunflower, peanut, and corn oil modified with MMT nanoparticles. |
| Scanning Electron Microscope | Produce high resolution images of MMT nanoparticles and wear scars of the block specimens. | Morphology of MMT nanoparticles and wear scars of the block specimens. |

| | | |
|---|---|---|
| XRD Spectroscopy | Identify the crystalline phases present in MMT nanoparticles. | Crystalline phases in MMT nanoparticles. |
| TA Instruments TGA Q500 | Determine the thermal stability of MMT nanoparticles. | Thermal degradation of MMT nanoparticles at a constant heating rate from 27°C to 1000°C . |
| Grizzly Milling Machine | Measure the torque acting on a specimen with the use of base sunflower, peanut, and corn oil modified with MMT nanoparticles. | Torque created using base sunflower, peanut, and corn oil modified with MMT nanoparticles. |
| Profilometer | Measure the roughness of the block samples before and after block-on-ring tests. | Average surface roughness for block samples after block-on-ring tests for base sunflower, peanut, and corn oil modified with MMT nanoparticles. |

State-of-the-Art Software

| Equipment | Purpose | Results Obtained |
|---|---|---|
| Vernier Logger Lite | Measure sensor data. | Gathered raw data as well as placing data into excel worksheets. |
| MATLAB | Simulation and analysis of results. | Fit rheology data into power law and Cross-equation models. Removed noise from the block-on-ring tests. |
| MS Office, i.e., Excel | Placing raw data into worksheets and plotting the data. | Figures required to analyze the data. |
| ImageJ | To measure the diameter size of MMT nanoparticles. | Average diameter of MMT nanoparticles. |
| Endnote | To manage reference citations during writing thesis or reports. | Reference citations during writing thesis report. |
| Origin | To plot the data. | Figures required to analyze the data. |

# BIOGRAPHICAL SKETCH

MD Mashfiqur Rahman has acquired his bachelor's degree in Mechanical Engineering from Bangladesh University of Engineering & Technology (BUET) in 2017 and joined the department of Mechanical Engineering at the University of Texas Rio Grande Valley in Spring 2020 for pursuing his master's degree. He worked as a graduate research assistant at the Mechanical Engineering Faculty Research Lab under Dr. Javier Ortega and completed his Master of Science in Mechanical Engineering in December 2021. His research interests are focused on nanomaterials, materials, tribology. During his Master's, he was awarded the Presidential Graduate Research Assistantship award for all two years. He has submitted one conference paper, one poster presentation, and is on the verge of submitting a journal. He got several offers for Ph.D. with full funding opportunity, and he is expected to join the Rensselaer Polytechnic Institute, Troy, NY in the Mechanical Engineering department. He can be reached at zisan.buet1210085@gmail.com.